TECHNICAL REPORT NO. NAS-1

Spreading Resistance As A Function Of Geometry And Frequency

February 1965

Contract No.: NAS 5-3546

Prepared by:

L. E. Dickens

The Johns Hopkins University
Carlyle Barton Laboratory
Charles and 34th Streets
Baltimore, Maryland 21218

For

NASA/Goddard Space Flight Center
Glenn Dale Road
Greenbelt, Maryland 20771

Copy No. 9

TECHNICAL REPORT NO. NAS-1

SPREADING RESISTANCE AS A FUNCTION OF GEOMETRY AND FREQUENCY

February 1965

Contract No.: NAS 5-3546

Prepared by:

L. E. Dickens

The Johns Hopkins University
Carlyle Barton Laboratory
Charles and 34th Streets
Baltimore, Maryland 21218

For

NASA/Goddard Space Flight Center
Glenn Dale Road
Greenbelt, Maryland 20771

FOREWORD

The author would like to express his appreciation of the support rendering possible this investigation. The supporting agencies are the National Aeronautics and Space Administration through Contract NAS 5-3546; and the Air Force Avionics Laboratory through contract AF 33(657)-11029. Acknowledgment goes also to Professors C. F. Miller and C. H. Palmer, Jr., who served as first and second referees respectively. The author would like also to thank Doctor J. M. Kopper for his review of the manuscript; Mrs. M. D. Denburg and Miss P. A. Shipley for numerical calculations and curve plotting; Mr. W. A. Ray and Mrs. N. L. Karweit for the programming of the calculations executed on the IBM 7094; Mr. C. M. LaPorte and Mr. R. H. Gordon for preparing the numerous figures; and last, but not least, Mrs. D. C. Scholl who carefully typed the manuscript.

ABSTRACT

The equivalent circuit applicable to most semiconductor diodes contains a term, R_s, called the spreading resistance which is a very critical parameter of any diode. In a mixer diode, R_s limits the conversion efficiency and increases the noise temperature. In parametric amplifiers, R_s affects the overall impedance levels and determines the minimum noise figure of which the amplifier is capable. In harmonic generators it drastically effects the conversion efficiency as it not only dissipates power at the input and output harmonic frequencies but also at every idler frequency for which current may flow through the diode.

R_s, of course, can be measured, but it is most important to be able to predict, before hand, the value of R_s for a given geometry as well as frequency. The geometrical variations are well demonstrated by calculations of R_s at low frequencies for which solutions of Laplace's equation hold. There calculations have been made, the computations having been performed on an IBM 7094 digital computer. The resistance of two typical configurations has been given for a wide range of geometries. The data has been presented in easily used graphical form.

Section III details more specifically the problems encountered when high frequency operation must be evaluated. The cylindrical capacitor is examined with emphasis on the configuration which applies to the variable capacitor diode which is used primarily for harmonic power generation.

The point contact diode configuration is examined and the field equations are derived in terms of the oblate spheroidal coordinates. It is shown that this is the natural coordinate system for such an analysis and that the spreading resistance is quite easily derived in this system.

TABLE OF CONTENTS

LIST OF ILLUSTRATIONS

LIST OF ILLUSTRATIONS CONTINUED

I. INTRODUCTION

The theme of this paper is the determination of the resistance encountered when a source of electricity makes contact through a (usually) flat disk electrode with a mass of conducting material which has located, at some distance from the disk, a sink of electricity. The reasons for pursuing such a subject is its direct applicability to the quantitative determination of the power-loss mechanisms of various semiconductor devices.

Semiconductor p-n junctions formed by solid-state diffusion, dot-alloy techniques, or other similar methods are relatively low loss nonlinear capacitors when properly biased. These diodes are used well into the microwave frequencies (1) to make low noise amplifiers, amplifying frequency converters, harmonic and sub-harmonic generators, switches, limiters, and voltage tunable passive circuits. As switches or protective devices, single junctions can control kilowatts of peak microwave power.

Point contact diodes as nonlinear resistors and nonlinear capacitors are similarly distinguished (2), (3). The point contact diode as a nonlinear resistor is as yet unchallenged as a microwave mixer or rectifier, and the point contact diode as a nonlinear capacitor has the potential (4) of much higher frequency operation as a low noise amplifier than the broad area junction devices.

Tunnel diodes are fabricated both by broad-area and by point-contact techniques. The tunnel diode is a very heavily doped semiconductor diode which exhibits a negative resistance characteristic over a small voltage range in the forward biased direction. Because of this negative resistance and an associated relatively low noise property the point contact tunnel diode has a strong potential application as a microwave amplifier and low level oscillator for frequencies well into the millimeter wave range.

The generally accepted (5) equivalent circuit of the junction, applicable to each of the above discussed semiconductor diodes by proper specification of the elements, is shown in Figure 1.

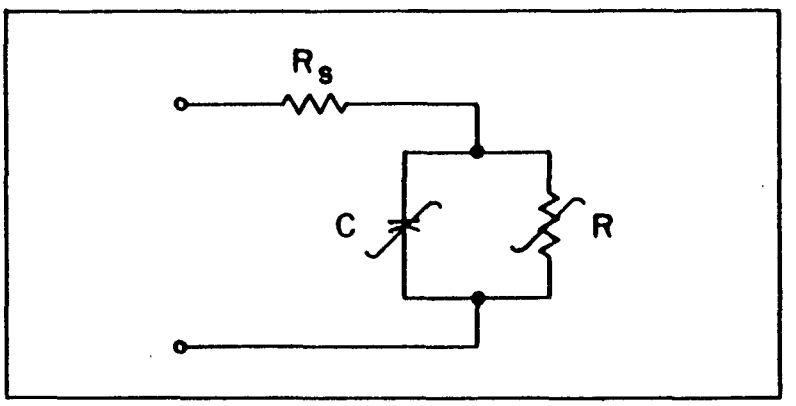

FIGURE 1 EQUIVALENT CIRCUIT OF THE JUNCTION OF A SEMICONDUCTOR DIODE.

The equivalent circuit consists of a nonlinear resistance R shunted by a nonlinear capacitance C, these two in series with a resistance R_s. R and C are nonlinear junction properties which

distinguish the mode of operation of the diode. When the diode is used as a variable reactance in a parametric amplifier, it is biased in the nonconducting region and the barrier resistance R becomes very high and thus negligible in comparison to the reactance of C. When the diode is used as a detector or mixer it is usually driven sufficiently far into the forward conducting region that R becomes much less than the reactance of C , and thus the C becomes negligible. The resistance R_s is the spreading resistance in the semiconductor resulting from the constriction of current flow lines in the semiconductor near the contact.

R_s exists and represents the loss mechanism for any diode. The determination of R_s under various conditions makes up the subject of this paper. The results may be extended to include the transistor diodes (base, emitter, collector).

The calculation of R_s becomes a problem with geometrical dependence, and, as skin effect will play a dominant role in the control of the flow of high frequency electric current, the calculations must accurately include this effect. In all the cases to be considered in the following sections cylindrical symmetry will be maintained in the device configuration as an aid to computation; however this imposes no limitations as it is a thoroughly practical assumption.

Section II of this paper deals with the steady flow of electric current in uniform isotropic media with the particularization of the treatment to the basic semiconductor diode configuration. The consideration of this type of potential problem is not new. Probably the first published consideration of this field was that by Weber (5) in 1873, from whose works Gray and Mathews (6) obtained many very instructive examples to demonstrate the application of Bessel functions to problems regarding the distribution of potential, and to the calculation of the resistance between source and sink located within an isotropic medium. Later the subject of the resistance of electric contacts (7, 8) became important as industry began making use of such devices as circuit breakers, relays, terminals, commutators, etc. The opening of the field of welding generated renewed interest in the determination of contact resistance (9, 10). Now the use of semiconductor diodes has created some rather particular problems. There exist many aspects of semiconductor device design (11) which present problems involving spreading resistance for which no elementary solution has yet been obtained.

Section III presents the theory of skin effect as it applies to parametric (capacitor) diodes and point-contact diodes. Most

references give no more than a passing glance at the subject of skin effect; thus, credit must be given to the text (12) by King on Electromagnetic Engineering which is most notable for its completeness.

II. ZERO FREQUENCY SPREADING RESISTANCE

This section begins with a review of the classical problems as presented by Weber. On this foundation are then constructed the problems of the semiconductor diodes encountered at frequencies sufficiently low that the skin effect has not yet set in.

A. CLASSICAL EXAMPLES

The simplest case, but one which is quite applicable to the problem of contact resistance, is that of the spherical contact imbedded in an infinite space of conductivity σ. As the space is infinite in extent and the only disturbance within the space is the source of potential, a perfectly conducting sphere of radius a, then, if the potential of the sphere be V_o, the potential at a distance r is

$$V = \frac{a}{r} V_o \quad . \tag{1}$$

Let the current density be $J = -\sigma \nabla V$, then at any radial distance r

$$J = \frac{\sigma a V_o}{r^2} \quad . \tag{2}$$

The total current flowing into or away from the sphere is

$$I_T = 4\pi a^2 J_o \quad , \tag{3}$$

where J_o is the current density evaluated at r = a. The resistance between the source, the perfectly conducting sphere, and the sink at infinity is just

$$R = \frac{V_o}{I_T} = \frac{1}{4\pi\sigma a} \quad . \tag{4}$$

Now consider Figure 2.

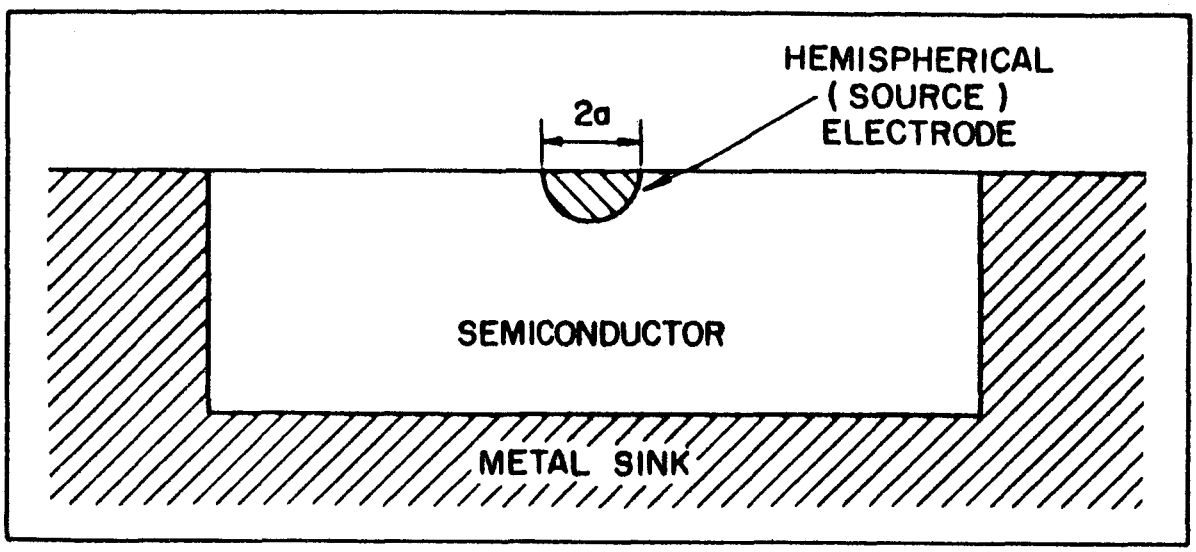

FIGURE 2 CASE OF HEMISPHERICAL CONTACT TO SEMICONDUCTOR.

If the radius of the source electrode is a and the electrode at a distance great in comparison with a from any part of the metal sink, then for this limiting case the resistance will be double that given by (4). In this case, the first applicable example of spreading resistance,

$$R_s = \frac{1}{2\pi\sigma a} \quad . \tag{5}$$

The next case to be examined is that of a circular disk contact of radius a upon an infinite half-space. (G&M)[1] gives an integral

---

1 G&M - Gray and Mathews - abbreviation used here and later to mean reference (6).

form for the potential distribution in the infinite half-space below the disk. If the disk be perfectly conducting, if $\underline{z}$ be taken along the axis of the disk, and the origin at the center,

$$V = \frac{2V_o}{\pi} \int_o^\infty e^{+\lambda z} \sin(\lambda a) J_o(\lambda r) \frac{d\lambda}{\lambda} \tag{6}$$

where V_o is the disk potential, and V is the potential at any point (r, z). $J_o(X)$ is the zero order Bessel function.

Justification for (6) can be briefly given as follows. Laplace's equation $\nabla^2 V = 0$, which must surely hold, is given in cylindrical coordinates as

$$\frac{\partial^2 V}{\partial r^2} + \frac{1}{r} \frac{\partial V}{\partial r} + \frac{1}{r^2} \frac{\partial^2 V}{\partial \theta^2} + \frac{\partial^2 V}{\partial z^2} = 0 \quad . \tag{7}$$

By symmetry considerations

$$\frac{\partial^2 V}{\partial \theta^2} = 0 \quad . \tag{8}$$

Then, if we set $V = RZ$, it can be seen that by separation of variables and setting

$$\frac{1}{Z} \frac{\partial^2 Z}{\partial z^2} = -\lambda^2 \tag{9}$$

and

$$\frac{1}{R} \left(\frac{\partial^2 R}{\partial r^2} + \frac{1}{r} \frac{\partial R}{\partial r}\right) = \lambda^2 \quad , \tag{10}$$

solutions for V can be written in the form

$$V = e^{\pm \lambda z} J_o(\lambda r) \quad , \tag{11}$$

in which form the integral is given, thus satisfying Equation (7). To show that $V = V_o$ on $r \leq a$ and $z = 0$, set $z = 0$ in Equation (6) and obtain

$$V(z = 0) = \frac{2V_o}{\pi} \int_o^\infty \sin(\lambda a)\, J_o(\lambda r)\, \frac{d\lambda}{\lambda} \quad . \tag{12}$$

But (G&M) (p. 126) evaluates the integral of (12) as

$$\int_o^\infty \sin(\lambda a)\, J_o(\lambda r)\, \frac{d\lambda}{\lambda} = \frac{\pi}{2} \text{ if } r < a \tag{13}$$

$$= \sin^{-1}\left(\frac{a}{r}\right) \text{ if } r > a \tag{14}$$

and as the results of (13) and (14) coincide for $r = a$ we have the fact that $V = V_o$ for $r \leq a$, $z = 0$.

Now to find the resistance between the disk electrode and the sink at infinity, the current density must be obtained. Again by use of

$$J = -\sigma \nabla V \tag{15}$$

there is obtained

$$J = -\frac{2\sigma V_o}{\pi} \int_o^\infty e^{\lambda z} \sin(\lambda a)\, J_o(\lambda r)\, d\lambda \, , \tag{16}$$

but again G&M (p. 73) present the integral evaluated for $z = 0$

$$\int_o^\infty \sin(\lambda a)\, J_o(\lambda r)\, d\lambda = 0 \quad \text{if } r^2 > a^2 \tag{17}$$

$$= \frac{1}{\sqrt{a^2 - r^2}} \text{ if } a^2 > r^2 \tag{18}$$

and then on the disk the current density is J_o.

$$J_o = - \frac{2\sigma V_o}{\pi \sqrt{a^2 - r^2}} \quad . \tag{19}$$

The total current, I_T, flowing through (or into) the disk is obtained by integrating the current density over the area of the disk; hence,

$$I_T = - 4\sigma V_o a \quad , \tag{20}$$

and in terms of total current, the current density on the disk is

$$J_o = \frac{I_T}{2\pi a \sqrt{a^2 - r^2}} \quad . \tag{21}$$

The negative sign in (20) simply implies that current flows in the negative $\underline{z}$ direction.

The resistance between the source electrode and the sink at infinity is then

$$R = \frac{1}{4\sigma a} \quad . \tag{22}$$

Now examine the following figure.

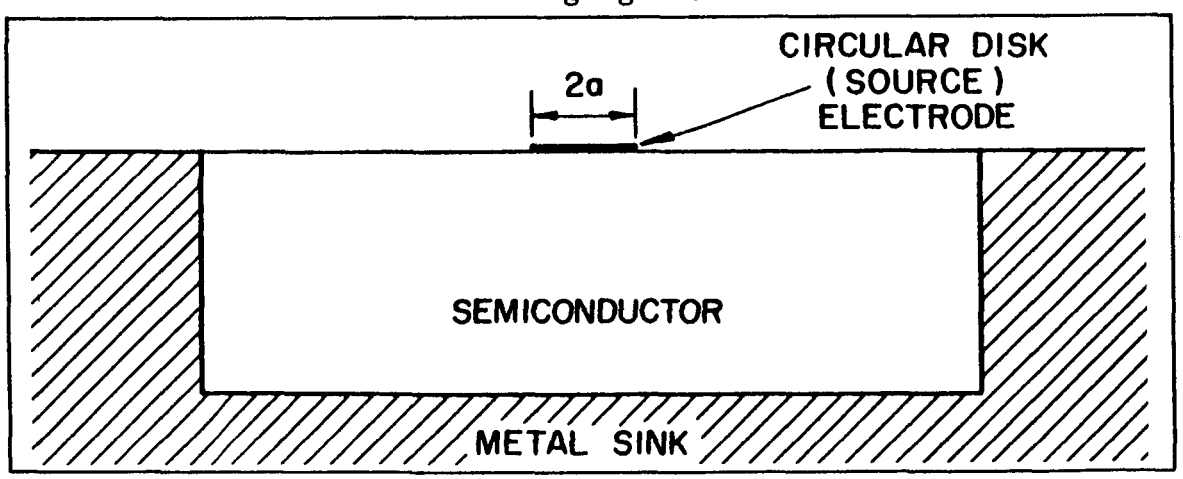

FIGURE 3 CASE OF THE FLAT CIRCULAR CONTACT TO SEMICONDUCTOR.

If we take the radius of the source electrode to be a and the electrode at a distance great in comparison with a from any part of the metal sink, then for this limiting case the resistance will be essentially that given by (22). Thus in this case, the second applicable example of spreading resistance R_s,

$$R_s = \frac{1}{4\sigma a} \quad . \tag{23}$$

This is the expression for spreading resistance most often encountered in the literature. Note that there is only a $(\pi/2)$ multiplicative factor difference between the value of R_s for the flat circular disk and the value of R_s for the hemispherical contact.

B. CYLINDRICAL SEMICONDUCTOR COMPONENTS

The above given examples are classical problems to which most authors refer, and the formulas for R_s of Equations (5) and (23) are those most often presented as representing the spreading resistance of point contact devices.

Many, if not most, problems associated with semiconductor diodes, and this includes the transistor diodes (base, emitter, collector), are not usually subject to the assumption of contact so small that the space below can be considered the infinite half space. Another assumption that cannot be made (even though low frequency operation is assumed) is that the disk is an equipotential. The usual forward biased diode may allow this

assumption, but consider the parametric (varactor) diode which is the p-n junction in reverse bias condition, as shown in the Figure 4. The depletion layer is the effective "width" of the capacitor, and is very small ($\approx$ 1000Å). As will be shown later, the contact disk may be a constant potential V_o, but contrary to Equation (21) the current density entering the space below the junction (depletion layer) will be uniform.

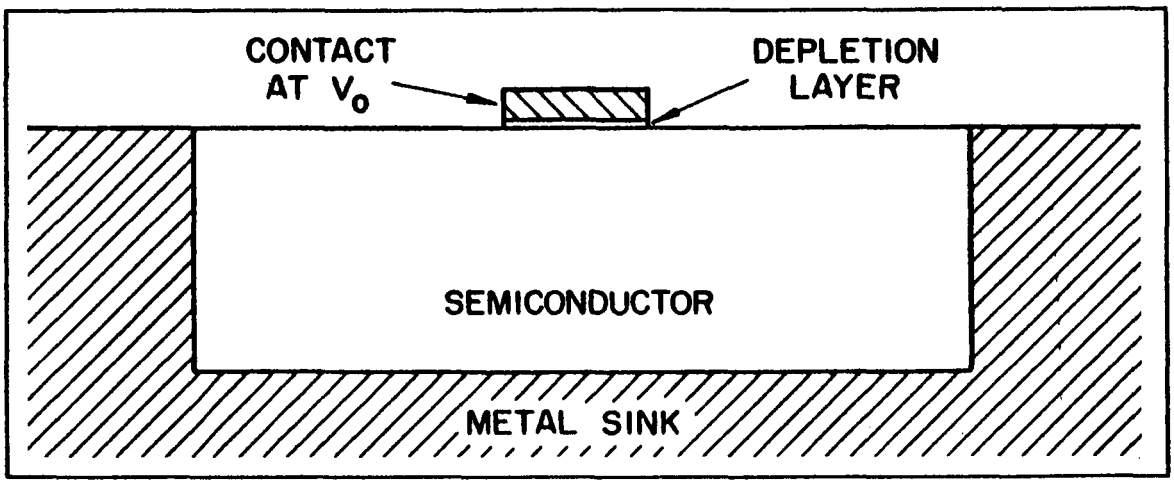

FIGURE 4 CAPACITOR CONTACT TO SEMICONDUCTOR.

This means that not only must we contend with a surface of constant potential and varying (in r) current density but also with a surface of constant current density and varying potential.

An approach to the solution with constant current density was made by Kennedy (11) who obtained the correct potential

distributions but then by using a definition of questionable accuracy[2] for the resistance, did not obtain the proper term for the spreading resistance.

Kennedy (11) gives the additional example for constant current density to be that of the mesa transistor, illustrated in Figure 5,

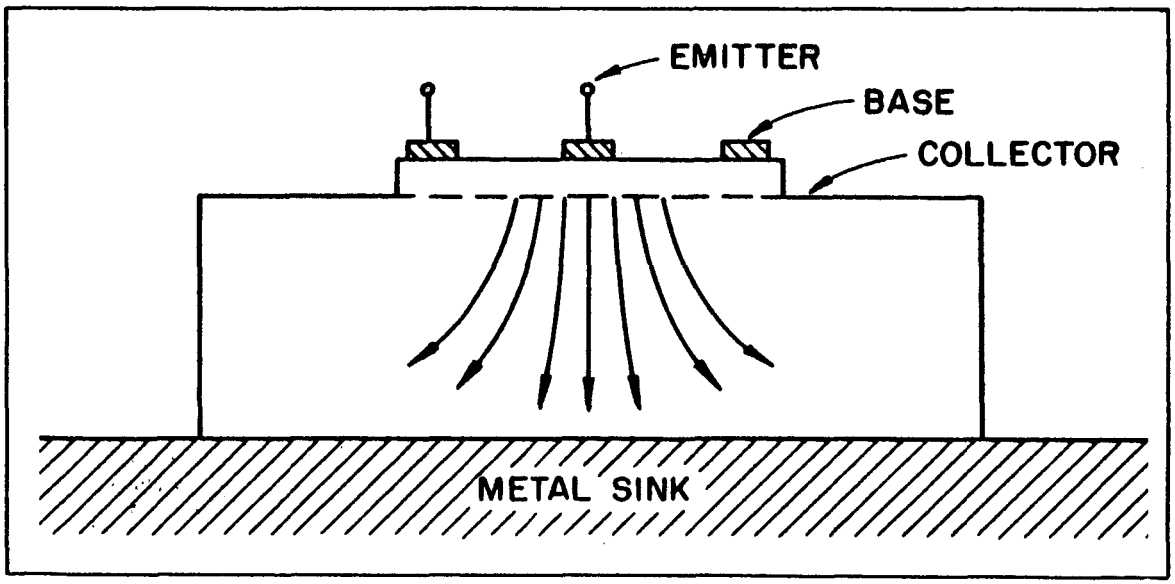

FIGURE 5 MESA CONSTRUCTION SHOWING ELECTRIC CURRENT SPREADING IN EXTRINSIC COLLECTOR REGION.

which he states has a radius of constant current density approximately equal to the emitter radius because there exists negligible minority carrier spreading within the base region.

---

2. Kennedy (in calculating the analogous thermal resistance) uses the definition: the ratio of the maximum cylinder temperature (potential) which appears at the center of its circular source to the total heat (current) entering this cylindrical conductor.

It is instructive and therefore beneficial to elaborate the steps to the solution of the boundary value problem in cylindrical coordinates that is here encountered.

A complete solution of Laplace's equation in cylindrical coordinates is of the form

$$V(r, z) = C_1 + C_2 z + (C_3 e^{\lambda z} + C_4 e^{-\lambda z}) J_o(\lambda r) \quad . \qquad (24)$$

Note that solutions involving the Neumann functions are not considered, as $V(0, z)$ must be finite, and that the cylindrical symmetry ($\partial V/\partial\theta = 0$) has already been imposed.

Let the configurations to be examined take the following form.

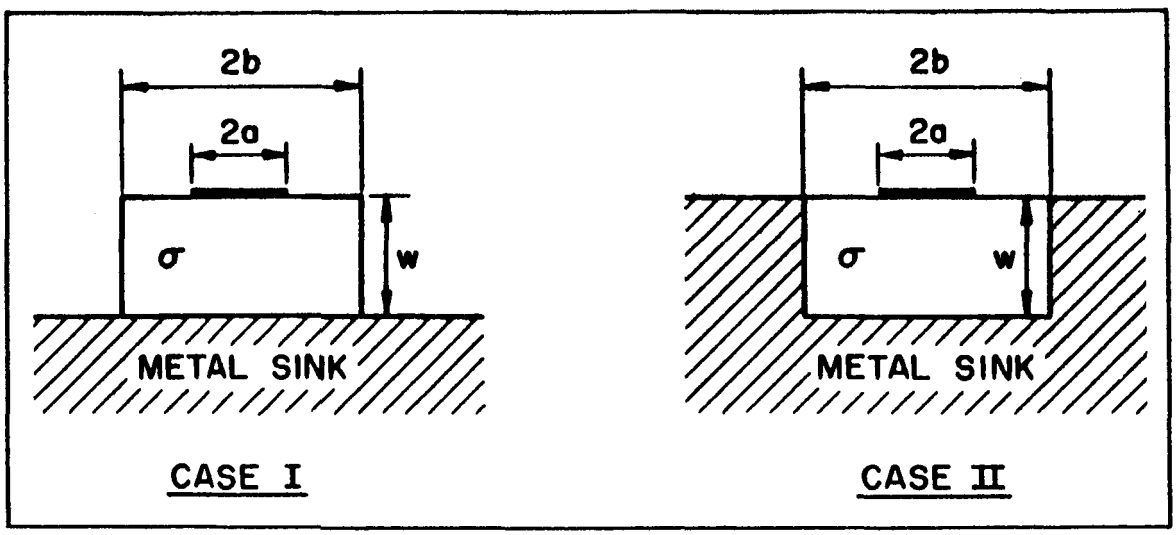

FIGURE 6 BASIC MODELS TO BE ANALYZED.

It is assumed that the semiconductor of conductivity σ is in contact with a high conductance return portion of the system. Thus for Case I we can assume the surface ($z = -w$, $0 < r < b$) and

for Case II the surfaces ($r = b$, $-w < z < 0$; and $0 < r < b$, $z = -w$) to be essentially at constant potential so that the tangential components of the electric intensity will be zero at the boundary. This causes the current flow lines to be perpendicular to these surfaces and allows the following conditions on $V(r, z)$

Case I
$$\frac{\partial V(r,z)}{\partial r} = 0 \qquad r = b \qquad -w < z < 0 \tag{25}$$

$$V(r,z) = 0 \qquad 0 < r < b \qquad z = -w \tag{26}$$

$$\frac{\partial V(r,z)}{\partial z} = \begin{cases} -\frac{1}{\sigma} J(r) & 0 < r < a \quad z = 0 \\ 0 & a < r < b \quad z = 0 \end{cases} \tag{27}$$

Case II
$$V(r,z) = 0 \qquad r = b \qquad -w < z < 0 \tag{28}$$

$$V(r,z) = 0 \qquad 0 < r < b \qquad z = -w \tag{29}$$

$$\frac{\partial V(r,z)}{\partial z} = \begin{cases} -\frac{1}{\sigma} J(r) & 0 < r < a \quad z = 0 \\ 0 & a < r < b \quad z = 0 \end{cases} \tag{30}$$

Notice that the condition on $\partial V/\partial z$ has been left as a function of $J(r)$, the current density at the contact surface. For the case taken by Kennedy, $J(r)$ is taken to be constant and no difficulty is encountered. But as $J(r)$ is left unspecified, for the moment, we have the much more difficult "mixed" boundary value problem. Smythe (13) presents an approximation to the solution of this problem for some particular values of (a/b) ratio (see Figure 6) and gives a measure of the "goodness" of the solutions by giving the magnitude of the deviation of the equipotential from the surface of the disk electrode. Smythe's solutions are restricted to Case I. An Appendix to Sackett's paper (9) gives a derivation by Roess which follows a similar form, and in each case, for actual results,

the density function of Equation (21) is used and the error in so using this function is then given in terms of the deviation of the equipotential from the disk, or the variation of the disk potential itself.

Case I: Applying the boundary conditions of (25), (26), and (27) to (24) yields

$$V_I(r,z)=\frac{(w+z)I_T}{\sigma\pi b^2}+\frac{2}{\sigma b}\sum_{n=1}^{\infty}\left[\int_o^a J(r)J_o(a'_n\frac{r}{b})rdr\right]\frac{\sinh\left[a'_n\frac{(z+w)}{b}\right]J_o(a'_n\frac{r}{b})}{\cosh(a'_n\frac{w}{b})(a'_n)J_o^2(a'_n)}, \quad (31)$$

where

$$I_T=\int_o^a J(r)\,2\pi dr \quad , \quad (32)$$

and the form of J(r) is as yet unspecified. Also note that a'_n is the n th root of $J_1(X)=0$, just as a_n^o is the n th root of $J_o(X)=0$.

Case II: Applying the boundary conditions of (28), (29), and (30) to (24) we obtain

$$V_{II}(r,z)=\frac{2}{\sigma b}\sum_{n=1}^{\infty}\left[\int_o^a J(r)J_o(a_n^o\frac{r}{b})rdr\right]\frac{\sinh\left[a_n^o\frac{(z+w)}{b}\right]J_o(a_n^o\frac{r}{b})}{\cosh(a_n^o\frac{w}{b})(a_n^o)J_1^2(a_n^o)} \quad . \quad (33)$$

Now Equations (31) and (33) represent exactly the potential distributions for the two cases. It is at this point that the approximations must be brought in. If J(r) is taken to be the constant distribution then V(r, z) is obtained exactly. But if the equipotential is stipulated over the disk electrode then we must use either Equation (21) or a modification thereof to represent J(r).

Now if we take Equation (21) to be representative of the current distribution associated with the equipotential across the disk electrode we are essentially supposing the return surfaces (of potential zero) sufficiently distant so that they do not disturb the current flow in the neighborhood of the disk electrode. The limits to this assumption must be examined carefully as it is obvious that, for Case I, as the ratio (a/b) approaches unity, then J(r) must approach the constant current density in the limit. Likewise, as the ratio (w/b) becomes very small, fringing effects at the electrode edges becomes negligible and the current density again is expected to become constant and independent of the radius.

Thus, the approach to be taken will be to evaluate the potentials and then the spreading resistance for the two cases and the two conditions on J(r) and present a "composite" set of data which satisfies all the known data or limit points.

If Equation (21) is substituted for J(r) into Equations (31) and (33) the spatial distribution of potential is obtained.[3] Then $V_I^e(r,z)$ becomes (superscript e is used to indicate electrode equipotential)

$$V_I^e(r,z)=\frac{I_T}{\pi a\sigma}\left\{\frac{a}{b}\left(\frac{w}{b}+\frac{z}{b}\right)+\sum_{n=1}^{\infty}\frac{\sinh\left[\alpha'_n\left(\frac{z}{b}+\frac{w}{b}\right)\right]J_o\left(\alpha'_n\frac{r}{b}\right)\sin\left(\alpha'_n\frac{a}{b}\right)}{\cosh\left(\alpha'_n\frac{w}{b}\right)\left(\alpha'_n\right)^2J_o^2\left(\alpha'_n\right)}\right\} \qquad (34)$$

and $V_{II}^e(r,z)$ becomes

---

3 The integral encountered in this substitution was evaluated by Sackett (p. 42) as

$$I=\int_o^a\frac{rJ_o\left(\lambda_n\frac{r}{b}\right)dr}{\left[1-\frac{r^2}{a^2}\right]^{1/2}}=\frac{ab}{\lambda_n}\sin\left(\lambda_n\frac{a}{b}\right).$$

$$V_{II}^{e}(r,z) = \frac{I_T}{\pi a \sigma} \sum_{n=1}^{\infty} \frac{\sinh\left[a_n^o\left(\frac{z}{b} + \frac{w}{b}\right)\right] J_o\left(a_n^o \frac{r}{b}\right) \sin\left(a_n^o \frac{a}{b}\right)}{\cosh\left(a_n^o \frac{w}{b}\right) (a_n^o)^2 J_1^2(a_n^o)} \quad . \tag{35}$$

The equations representing the potentials for the two cases, for the assumption of constant electrode current density, are $V_I^c(r,z)$ and $V_{II}^c(r,z)$, where the superscript c is used to denote constant electrode current density, which will be taken to be $J(r) = I_T/\pi a^2$. Hence, for the integral in Equations (31) and (33) we have

$$\int_o^a J(r)\, J_o\left(a_n \frac{r}{b}\right) r\,dr = \left(\frac{b}{a}\right) \frac{I_T}{\pi a_n} J_1\left(a_n \frac{a}{b}\right) \quad , \tag{36}$$

and then from Equation (31) we obtain

$$V_I^c(r,z) = \frac{I_T}{\pi \sigma a} \left\{ \frac{a}{b}\left(\frac{w}{b} + \frac{z}{b}\right) + 2 \sum_{n=1}^{\infty} \frac{\sinh\left[a_n'\left(\frac{z}{b}+\frac{w}{b}\right)\right] J_1\left(a_n' \frac{a}{b}\right) J_o\left(a_n' \frac{r}{b}\right)}{\cosh\left(a_n' \frac{w}{b}\right)(a_n')^2 J_o^2(a_n')} \right\}, \tag{37}$$

and from Equation (33) we obtain

$$V_{II}^c(r,z) = \frac{2I_T}{\pi \sigma a} \sum_{n=1}^{\infty} \frac{\sinh\left[a_n^o\left(\frac{z}{b} + \frac{w}{b}\right)\right] J_1\left(a_n^o \frac{a}{b}\right) J_o\left(a_n^o \frac{r}{b}\right)}{\cosh\left(a_n^o \frac{w}{b}\right)(a_n^o)^2 J_1^2(a_n^o)} \quad . \tag{38}$$

The spreading resistance R_s, has been defined as the total resistance to current of the matter between the disk electrode and the return surfaces (zero potential surfaces). For the equipotential case this resistance represents the I^2R losses (P_o) of the matter, and for the constant current density case it is only logical

to make the definition of spreading resistance to mean the resistance determined by the I^2R losses of the material, therefore we take to be the equivalent definition

$$R_s^e = \frac{V_o}{I_T} \quad \text{(Equipotential case)} \quad , \tag{39}$$

and

$$R_s^c = \frac{P_o}{I_T^2} \quad \text{(Constant electrode current density)}, \tag{40}$$

where I_T is given by Equation (32) to be the total current passing through the disk electrode, V_o is the potential of the disk electrode for the equipotential case, and P_o is the I^2R loss of the matter between the disk electrode and the return surfaces for the constant input current density case. As V_o, the equipotential of the disk given by Equations (34) and (35), has within the summation the $\underline{r}$ dependence, we can by the equivalence of formulas (39) and (40) use the I^2R concept most conveniently to dispose of this $\underline{r}$ dependence. Let P_o be given by the following equation,

$$P_o = \int_o^a V(r,0)\, J(r)\, 2\pi dr \quad ,$$

and by using Equation (40) we have

$$R_s = \frac{1}{I_T^2} \int_o^a V(r,0)\, J(r)\, 2\pi r dr \quad . \tag{41}$$

Then by substituting Equation (37) into (41), and normalizing to $R_{so} = 1/4\sigma a$ we have

$$\frac{R^{c}_{sI}}{R_{so}} = \frac{4}{\pi}\left\{\left(\frac{a}{b}\right)\left(\frac{w}{b}\right) + 4\left(\frac{b}{a}\right)\sum_{n=1}^{\infty}\frac{\tanh\left(a'_n\frac{w}{b}\right)J_1^2\left(a'_n\frac{a}{b}\right)}{(a'_n)^3 J_o^2(a'_n)}\right\}, \qquad (42)$$

and by using Equation (40) we obtain

$$\frac{R^{c}_{sII}}{R_{so}} = \frac{16}{\pi}\left(\frac{b}{a}\right)\sum_{n=1}^{\infty}\frac{\tanh\left(a^{o}_n\frac{w}{b}\right)J_1^2\left(a^{o}_n\frac{a}{b}\right)}{(a^{o}_n)^3 J_1^2(a^{o}_n)} \quad . \qquad (43)$$

For the equipotential case, by similar procedure we obtain

$$\frac{R^{e}_{sI}}{R_{so}} = \frac{4}{\pi}\left\{\left(\frac{a}{b}\right)\left(\frac{w}{b}\right) + \left(\frac{b}{a}\right)\sum_{n=1}^{\infty}\frac{\tanh\left(a'_n\frac{w}{b}\right)\sin^2\left(a'_n\frac{a}{b}\right)}{(a'_n)^3 J_o^2(a'_n)}\right\} \qquad (44)$$

and

$$\frac{R^{e}_{sII}}{R_{so}} = \frac{4}{\pi}\left(\frac{b}{a}\right)\sum_{n=1}^{\infty}\frac{\tanh\left(a^{o}_n\frac{w}{b}\right)\sin^2\left(a^{o}_n\frac{a}{b}\right)}{(a^{o}_n)^3 J_1^2(a^{o}_n)} \quad . \qquad (45)$$

Equations (42), (43), (44), and (45) now give, in normalized form and subject only to the limitation of the approximations as to current distribution, the spreading resistance of a wide variety of cylindrically symmetric configurations. The results from these equations have been obtained through their computation on an IBM 7094 digital computer. The data are presented in Figures 7, 8, 9, and 10.

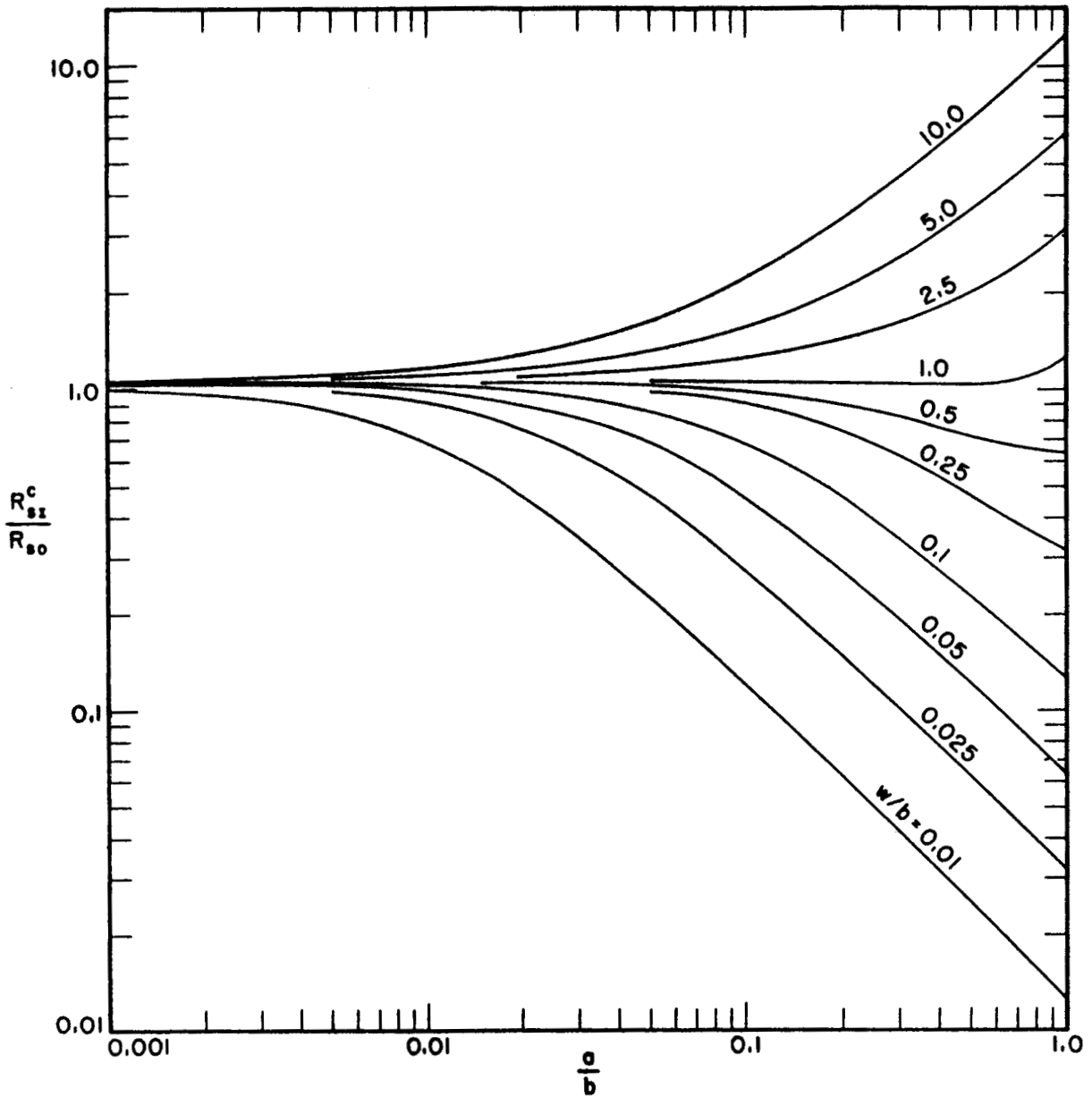

FIGURE 7 SPREADING RESISTANCE - ZERO FREQUENCY CONSTANT CURRENT DENSITY CONTACT: CASE I.

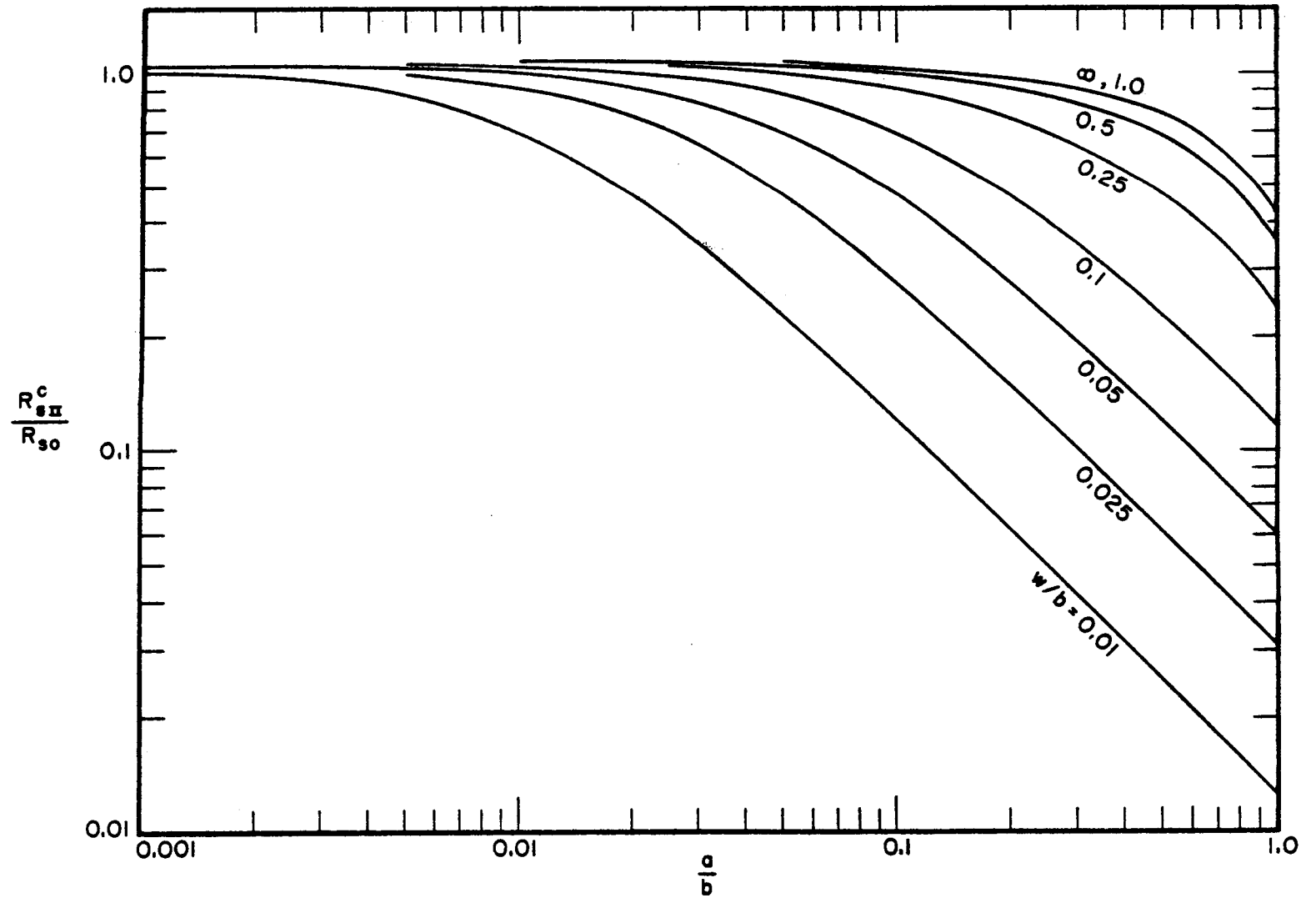

FIGURE 8 SPREADING RESISTANCE - ZERO FREQUENCY CONSTANT CURRENT DENSITY CONTACT: CASE II.

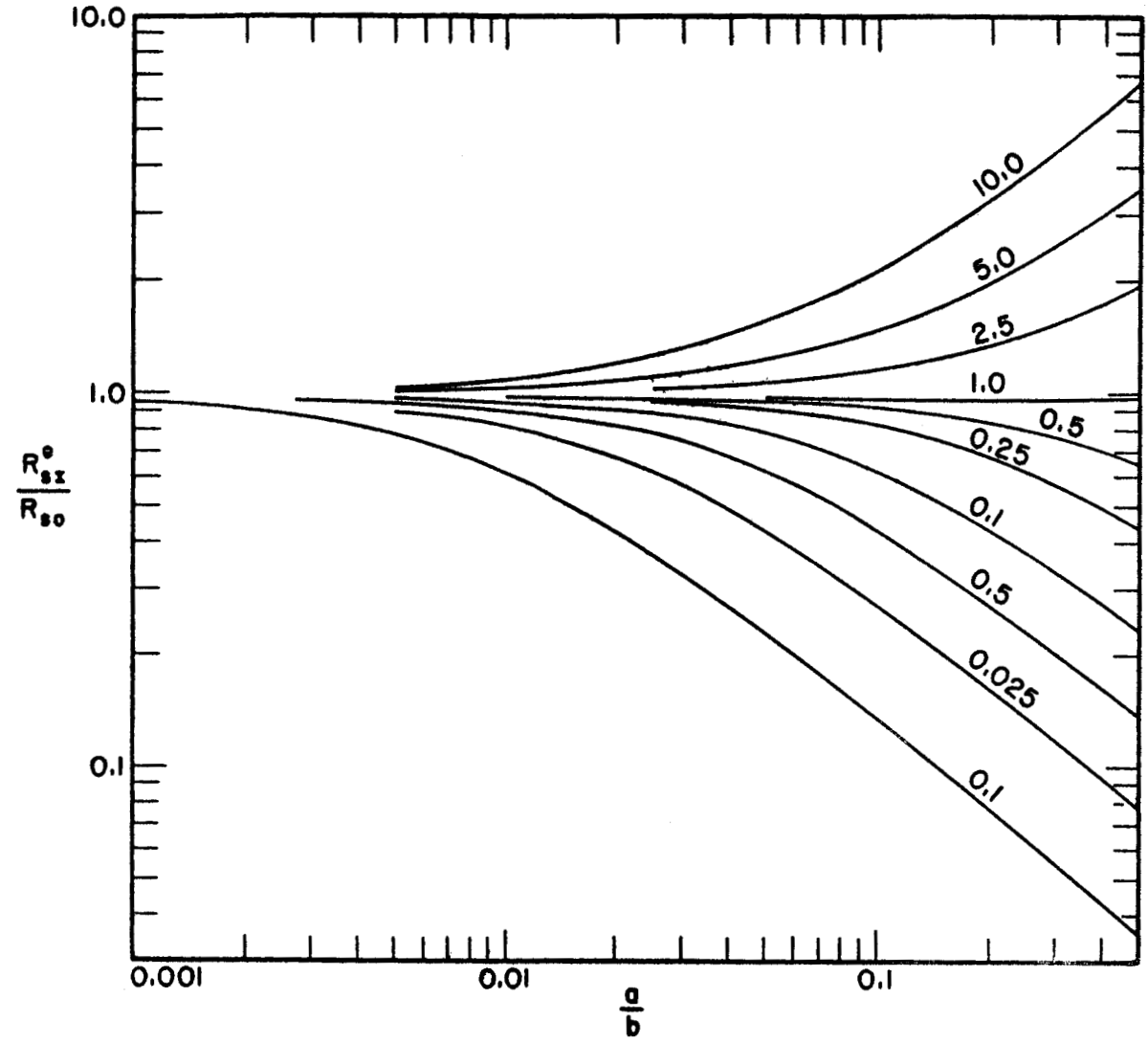

FIGURE 9 SPREADING RESISTANCE - ZERO FREQUENCY EQUIPOTENTIAL CONTACT: CASE I.

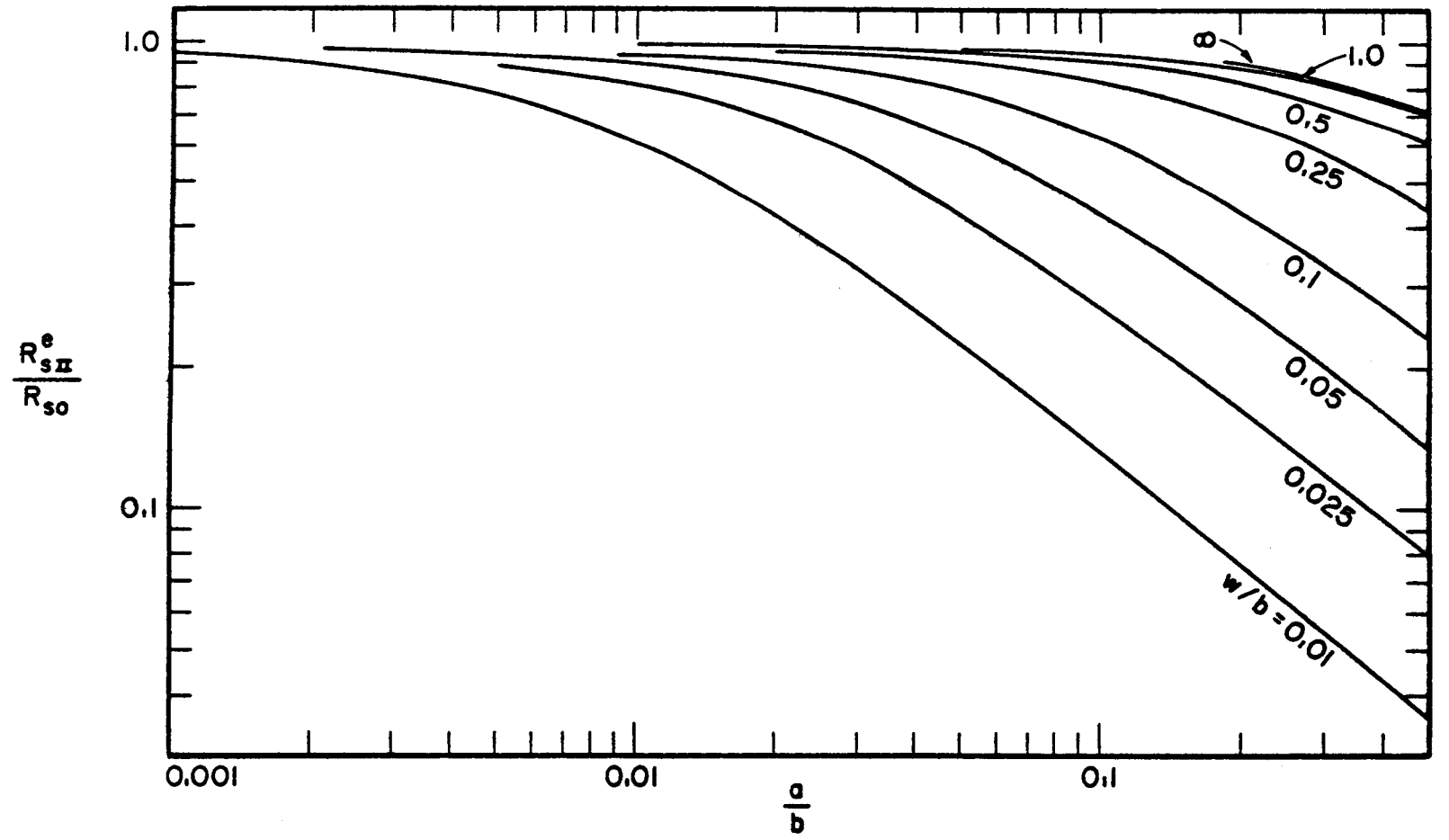

FIGURE 10 SPREADING RESISTANCE - ZERO FREQUENCY EQUIPOTENTIAL CONTACT: CASE II.

The data of these figures are subject to the assumption of either constant current density or the current density of the very small contact. The current density of most of the range of physical configuration takes on a characteristic somewhere between these two extremes.

In a real situation, neither assumption is completely valid. It is recognized that for both Cases I and II where (w/b) is small and (a/b) is only moderately large then fringing effects can be neglected and a constant current density must exist. Again, for Case I, when (a/b) goes to unity, it is easily seen that a constant current density must exist. On the other hand, for both Case I and II when (a/b) is small and (w/b) is moderately large then the assumed distribution of Equation (21) does hold. For Case I, the two assumed distributions represent the limiting situations for the current distribution and the resulting resistance values shown in Figure 11 (Composite: Case I) represent a smooth transition between the two values given in Figures 7 and 8. For Case II, as we have stated, the similar situation holds for all but the larger values of (a/b) ratio (hence the cut-off of the curves at the point (a/b) = 0.5) and the resistance values plotted in Figure 12 (Composite: Case II) represent a smooth transition between the corresponding values shown in Figures 9 and 10.

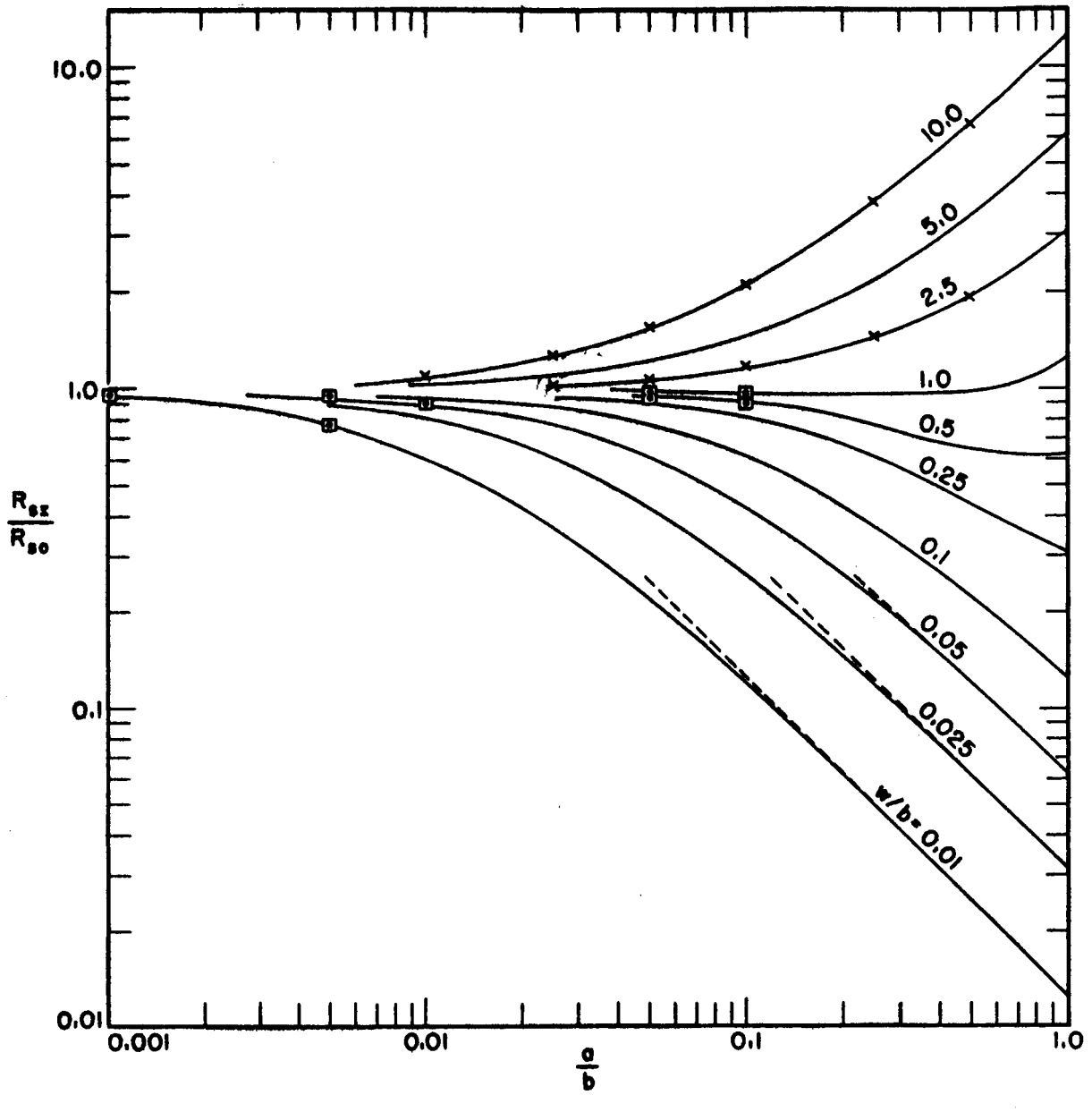

FIGURE 11 SPREADING RESISTANCE - ZERO FREQUENCY COMPOSITE CURVE; CASE I.

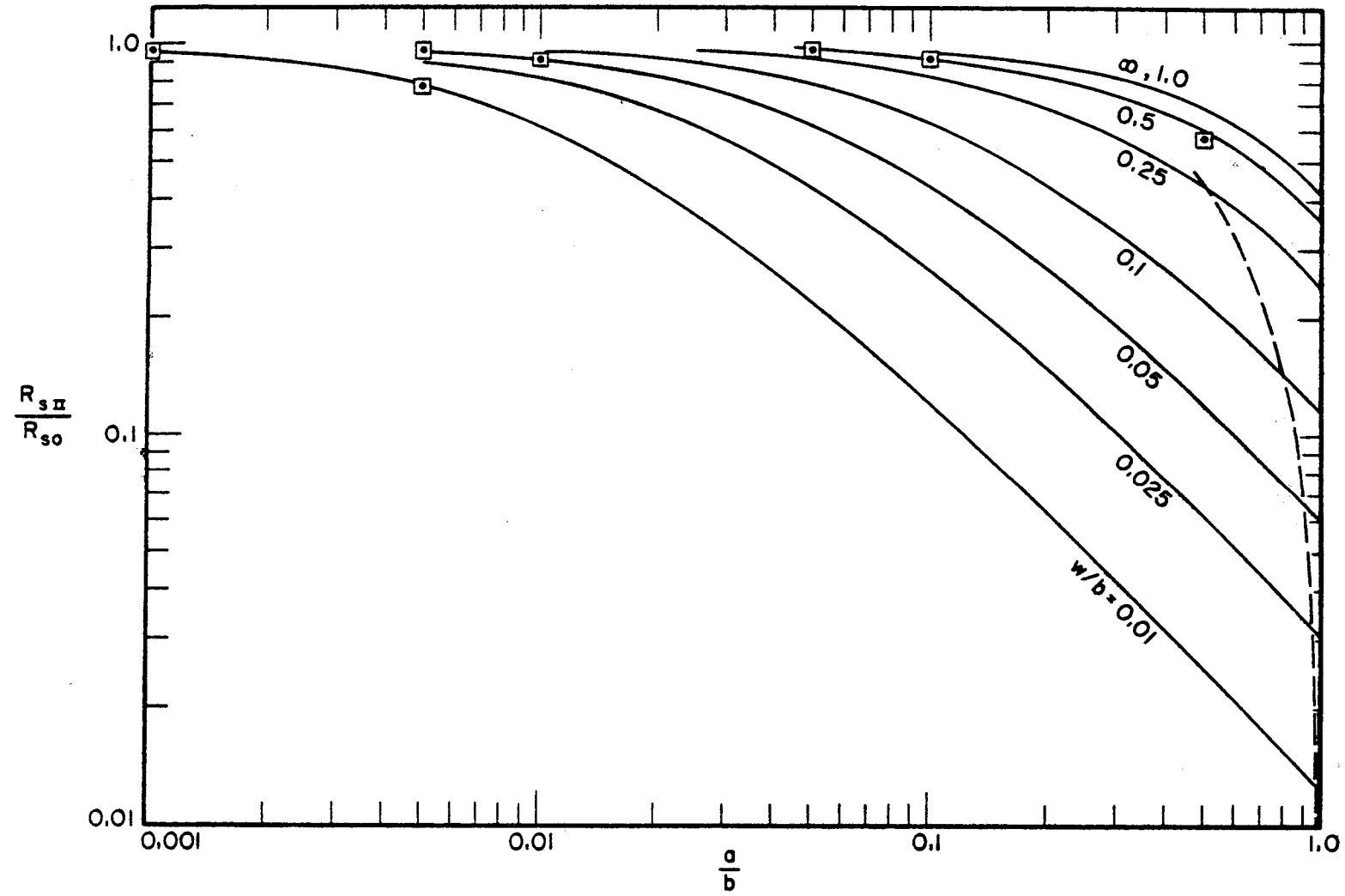

FIGURE 12 SPREADING RESISTANCE - ZERO FREQUENCY COMPOSITE CURVE: CASE II.

To justify the presentation of the data in the "composite" form, there are several approximations that can be used. The first is that of G&M (Chapter XII) which gives, in our own notation, the spreading resistance for small (a/b) and (w/b) ratios in Case I (equally valid for Case II) as

$$\frac{R}{R_{so}} = \left\{1 - \frac{a}{w}\left[\frac{2}{\pi}\ln 2 - 4e^{-\pi\left(\frac{w}{b}\right)}\right]\right\} \quad . \tag{46}$$

Several values were obtained by hand computation of this expression and the points plotted in Figures 11 and 12. The points are distinguished by the square enclosures.

The second expression used to check the composite curves is the polynomial approximation given by Roess (9) which was experimentally verified by Sackett (9). In our own notation this is, for Case I and $(w/b) \geq 1$

$$\frac{R_I}{R_{so}} = \frac{4}{\pi}\left(\frac{a}{b}\right)\left(\frac{w}{b}\right) + \left[1 - 1.40925\left(\frac{a}{b}\right) + 0.29591\left(\frac{a}{b}\right)^3 + \right.$$

$$\left. + 0.05254\left(\frac{a}{b}\right)^5 + 0.02105\left(\frac{a}{b}\right)^7\right] \tag{47}$$

Several values were obtained by hand computation and the points plotted in Figure 11. The points are distinguished by X's through the points.

When the ratio (w/b) is very small the resistance can be given as the resistance of a cylinder of length w and radius a modified by a factor, call it F, to include the effect of fringing. Then the normalized expression for the resistance is

$$\frac{R}{R_{so}} = \frac{4}{\pi}\left(\frac{w}{a}\right) F \quad . \tag{48}$$

Certainly, when the ratio (w/a) is very small, then F goes to unity. Further, it is true that for Case I, when (a/b) = 1, Equation (48) holds exactly. These conclusions are demonstrated in Figure 11. The dashed lines show how the resistance values do in fact approach the asymptotic values as required. For Case II, when the ratio (a/b) is small and (w/b) is likewise, then the same situation holds as just described. But there is a value for the ratio (a/b) above which the assumption of constant current no longer holds. Suppose that it be stipulated that the assumption is acceptable if the dimensions satisfy the bounds $a \geq 2w$ and $(b-a) \geq 2w$. In Figure 12 these bounds are satisfied by all the points lying to the left of the dashed line.

On the basis of these arguments, it appears that the composite curves of Figures 11 and 12 yield accurate values for the dc spreading resistance where the disk contact is a direct contact; that is, there exists no space charge at the contact, or other mechanism to distort the current distribution from that which would exist if the disk were not at a constant potential.

III. SKIN EFFECT AND RF IMPEDANCE

The constriction of current flow through a small disk electrode and the calculation of the resulting distribution is sufficiently complicated at zero frequency that the use of high speed computers is the only feasible way of obtaining any amount of data. This has already been demonstrated in previous sections. With the consideration of high frequency operation, one must consider the influence of skin effect[4] and the degree to which it forces the further constriction of the current to the outermost surfaces of the region of current flow.

A. FIELD EQUATIONS

As the current distributions maintain general rotational symmetry and in particular all configurations maintain cylindrical symmetry, all the formulas for the field will be derived subject to this restriction.

1. General Rotational Symmetry

Given the system of coordinates (ξ, η, θ) with rotational symmetry, the metrical coefficients are defined by the equation

$$ds^2 = h_1^2 d\xi^2 + h_2^2 d\eta^2 + r^2 d\theta^2 \qquad (49)$$

where r is the perpendicular distance from the axis of rotation. If the field has the same symmetry as the coordinate systems, its

4. Skin effect has been concisely defined by Holm (8): "The Effect consists of an induction by the currents own magnetic field pressing the lines of flow towards the exterior of the conductor, thus diminishing the effective conducting cross section and increasing the resistance."

components are independent of θ, and, following Stratton (14), one finds that

$$\text{curl } E = -j\omega\mu H \tag{50}$$

and

$$\text{curl } H = (\sigma + j\omega\epsilon)\, E = \frac{\gamma^2 E}{j\omega\mu} \tag{51}$$

break up into the following set (for $H = H_\theta \vec{\theta}$)

$$\frac{1}{rh_2} \frac{\partial}{\partial \eta} (rH_\theta) = \frac{+\gamma^2}{j\omega\mu} E_\xi \quad , \tag{52}$$

$$\frac{1}{rh_1} \frac{\partial}{\partial \xi} (rH_\theta) = \frac{-\gamma^2}{j\omega\mu} E_\eta \quad , \tag{53}$$

$$\frac{1}{h_1 h_2} \left[\frac{\partial}{\partial \xi} (h_2 E_\eta) - \frac{\partial}{\partial \eta} (h_1 E_\xi) \right] = -j\omega\mu H_\theta \quad , \tag{54}$$

and that these relations are satisfied by the scalar function Q which is defined as

$$Q = rH_\theta \quad . \tag{55}$$

Then, in terms of Q, the electric intensities are given as

$$E_\xi = \frac{j\omega\mu}{rh_2\gamma^2} \frac{\partial Q}{\partial \eta} \tag{56}$$

and

$$E_\eta = \frac{-j\omega\mu}{rh_1\gamma^2} \frac{\partial Q}{\partial \xi} \quad . \tag{57}$$

The resulting second order, linear, partial differential equation that is obtained is

$$\frac{\partial}{\partial \xi}\left(\frac{h_2}{r h_1}\frac{\partial Q}{\partial \xi}\right) + \frac{\partial}{\partial \eta}\left(\frac{h_1}{r h_2}\frac{\partial Q}{\partial \eta}\right) - \gamma^2 \frac{h_1 h_2}{r} Q = 0 \qquad (58)$$

2. Cylindrical Coordinates

Now if cylindrical symmetry is encountered so as to make desirable the use of the cylindrical coordinate system, we take $\xi = r$, the radial component; $\eta = z$, the axial component; and $\theta = \theta$, the angular component. The metrical coefficients are then $h_1 = h_2 = 1$, and $r = r$. The differential equation takes the form shown in Equation (59).

$$\frac{\partial^2 Q}{\partial r^2} - \frac{1}{r}\frac{\partial Q}{\partial r} + \frac{\partial^2 Q}{\partial z^2} - \gamma^2 Q = 0 \quad . \qquad (59)$$

Separation of variables is effected by the substitution of

$$Q(r, z) = Q(r)\, Q(z) \qquad (60)$$

into Equation (59). This operation yields the two equations

$$\frac{\partial^2 Q(z)}{\partial z^2} - k^2 Q(z) = 0 \qquad (61)$$

and

$$\frac{\partial^2 Q(r)}{\partial r^2} - \frac{1}{r}\frac{\partial Q(r)}{\partial r} - (\gamma^2 - k^2) Q(r) = 0 \quad , \qquad (62)$$

where γ is the intrinsic propagation constant and k is the separation constant.

The solution to Equation (61) is of the form

$$Q(z) = C\, e^{\pm kz} \quad , \tag{63}$$

where C is a scale factor to be determined by boundary conditions. The solution to Equation (62) is of the form[5]

$$Q(r) = C_1 r J_1(\beta r) + C_2 r N_1(\beta r) \quad , \tag{64}$$

where

$$\beta = \sqrt{k^2 - \gamma^2} \quad . \tag{65}$$

From Equations (56) and (57) the electric intensities are found to be

$$E_r = \frac{j\omega\mu}{\gamma^2} \frac{1}{r} \frac{\partial Q}{\partial z} \tag{66}$$

and

$$E_z = \frac{-j\omega\mu}{\gamma^2} \frac{1}{r} \frac{\partial Q}{\partial r} \quad . \tag{67}$$

As the electric intensities must be finite for r = 0, the Neumann function of Equation (64) is not allowed, hence $C_2 = 0$. Then, after substituting Equations (60), (63), and (64) into the formulas for E_r E_z, they obtain the form

$$E_r = \pm \frac{j\omega\mu}{\gamma^2} kr\, J_1(\beta r)\, e^{\pm kz}\, A_1 \tag{68}$$

and

$$E_z = - \frac{j\omega\mu}{\gamma^2} \beta\, J_o(\beta r)\, e^{\pm kz}\, A_2 \quad , \tag{69}$$

---

5. Reference (15), p. 146.

where again A_1 and A_2 are scale factors yet to be determined. Similarly the magnetic intensity, obtained from Equations (55) and (64), is found to have the form

$$H_\theta = A_3 J_1(\beta r) \quad . \tag{70}$$

B. CYLINDRICAL CONDUCTORS

This section consists briefly of two parts. First a classical example of a skin effect type of calculation is reviewed, and second the principles so discussed are applied in detail to the large area capacitor problem.

1. Classical Example - Long Cylindrical Conductor

For this case we consider the problem of the distribution of current in the interior of a long cylindrical conductor. Since we are assuming a long conductor, the variation of Q along the $\underline{z}$ axis can be taken to be zero (hence $k = 0$), which gives $E_r = 0$ by Equation (66) (or Equation (68)). If the cylinder is assigned the radius $r = a$, and if $E_z(a)$ is the $\underline{z}$ component of the electric intensity at the cylinder surface, it follows from Equation (69) that

$$E_z(r) = E_z(a) \frac{J_o(\beta r)}{J_o(\beta a)} \quad . \tag{71}$$

The current density is related to the electric intensity by

$$J_z(r) = (\sigma + j\omega\epsilon)\, E_z(r) \quad , \tag{72}$$

where σ is the bulk conductivity and ϵ the absolute dielectric constant (permittivity) of the conducting medium. The current density $J_z(r)$, for any $\underline{r}$ within the cylinder, is given in terms of $E_z(a)$ to be

$$J_z(r) = (\sigma + j\omega\epsilon)\, E_z(a) \frac{J_o(\beta r)}{J_o(\beta a)} \quad , \tag{73}$$

from which is obtained the total current, I_T, flowing in the cylinder.

$$I_T = 2\pi a(\sigma + j\omega\epsilon)\, E_z(a) \frac{J_1(\beta a)}{\beta J_o(\beta a)} \quad . \tag{74}$$

Now the impedance per unit length, Z_ℓ, of the long cylinder can be given as

$$Z_\ell = \frac{E_z(a)}{I_T} \tag{75}$$

in ohms per unit length, hence

$$Z_\ell = \frac{\beta J_o(\beta a)}{2\pi a(\sigma + j\omega\epsilon) J_1(\beta a)} \quad . \tag{76}$$

As $k = 0$, $\beta = j\gamma$ is substituted in Equation (76), and for this situation the following formula obtains,

$$Z_\ell = \frac{-\omega\mu}{2\pi\gamma a} \frac{J_o(j\gamma a)}{J_1(j\gamma a)} \quad . \tag{77}$$

If it be assumed that the cylinder is a relatively good conductor, we can put

$$j\gamma = j\sqrt{j\omega\mu\sigma} \quad = -(1 - j)\sqrt{\frac{\omega\mu\sigma}{2}} \quad . \tag{78}$$

Define the parameter

$$d = \sqrt{\frac{2}{\omega\mu\sigma}} \quad , \tag{79}$$

and there holds by Equations (77) and (78), the relation

$$Z_\ell = \frac{\omega\mu}{2\pi\gamma a} \quad \frac{J_o\left[(1-j)\frac{a}{d}\right]}{J_1\left[(1-j)\frac{a}{d}\right]} \quad . \tag{80}$$

If the ratio $(a/d) \gg 1$, we may substitute for $J_o(X)$ and $J_1(X)$ the following approximating expressions

$$J_o\left[(1-j)\frac{a}{d}\right] \doteq \frac{1}{4\sqrt{2}}\sqrt{\frac{d}{2\pi a}}\; e^{\frac{a}{d}(1+j) - j\frac{\pi}{8}} \quad , \tag{81}$$

$$J_1\left[(1-j)\frac{a}{b}\right] \doteq \frac{1}{4\sqrt{2}}\sqrt{\frac{d}{2\pi a}}\; e^{\frac{a}{d}(1+j) - j\frac{5\pi}{8}} \tag{82}$$

and thus obtain the much simpler expression for Z_ℓ,

$$Z_\ell = \frac{(1+j)}{2\pi a}\sqrt{\frac{\omega\mu}{2\sigma}} \quad . \tag{83}$$

Note that Equation (73) could have been written as

$$J_z(r) = J_z(a)\,\frac{J_o(\beta r)}{J_o(\beta a)} \quad , \tag{84}$$

then, as was done in Equation (77), the approximation of Equations (81) and (82) yield

$$J_z(r) = J_z(a)\, e^{-\frac{u}{d}(1+j)} \quad , \tag{85}$$

where u is taken as the penetration toward the center of the cylinder and is a positive number. When u = d, the current density, $J_z(r)$, has been reduced by a factor e^{-1} hence d is the classically defined skin depth d_s, and the previously assigned condition $(a/d) >> 1$ states that this radius of the cylinder is large with respect to a skin depth. If these conditions be satisfied then the real and imaginary parts of Z_ℓ are equal, and if

$$Z_\ell = R_\ell + jX_\ell \quad , \tag{86}$$

then

$$R_\ell = X_\ell = \frac{1}{2\pi a}\sqrt{\frac{\omega\mu}{2\sigma}} \quad , \tag{87}$$

and by Equation (79) with the identification, $d = d_s$ we have

$$R_\ell = X_\ell = \frac{1}{2\pi a d_s \sigma} \quad . \tag{88}$$

Equation (87) is called the Rayleigh formula[6]. Equation (88) shows the resistance per unit length of the conducting cylinder to be inversely proportional to the area of an annulus of very small width, d_s, and circumference $2\pi a$. This is consistent with the fact that the current predominantly flows in a skin of thickness d_s on the surface of the cylinder when γa is large. Various values of σ (or $\rho = 1/\sigma$) were used, and a broad range of values of d_s versus frequency are shown in Figure 13.

---

6. Reference (12), p. 348.

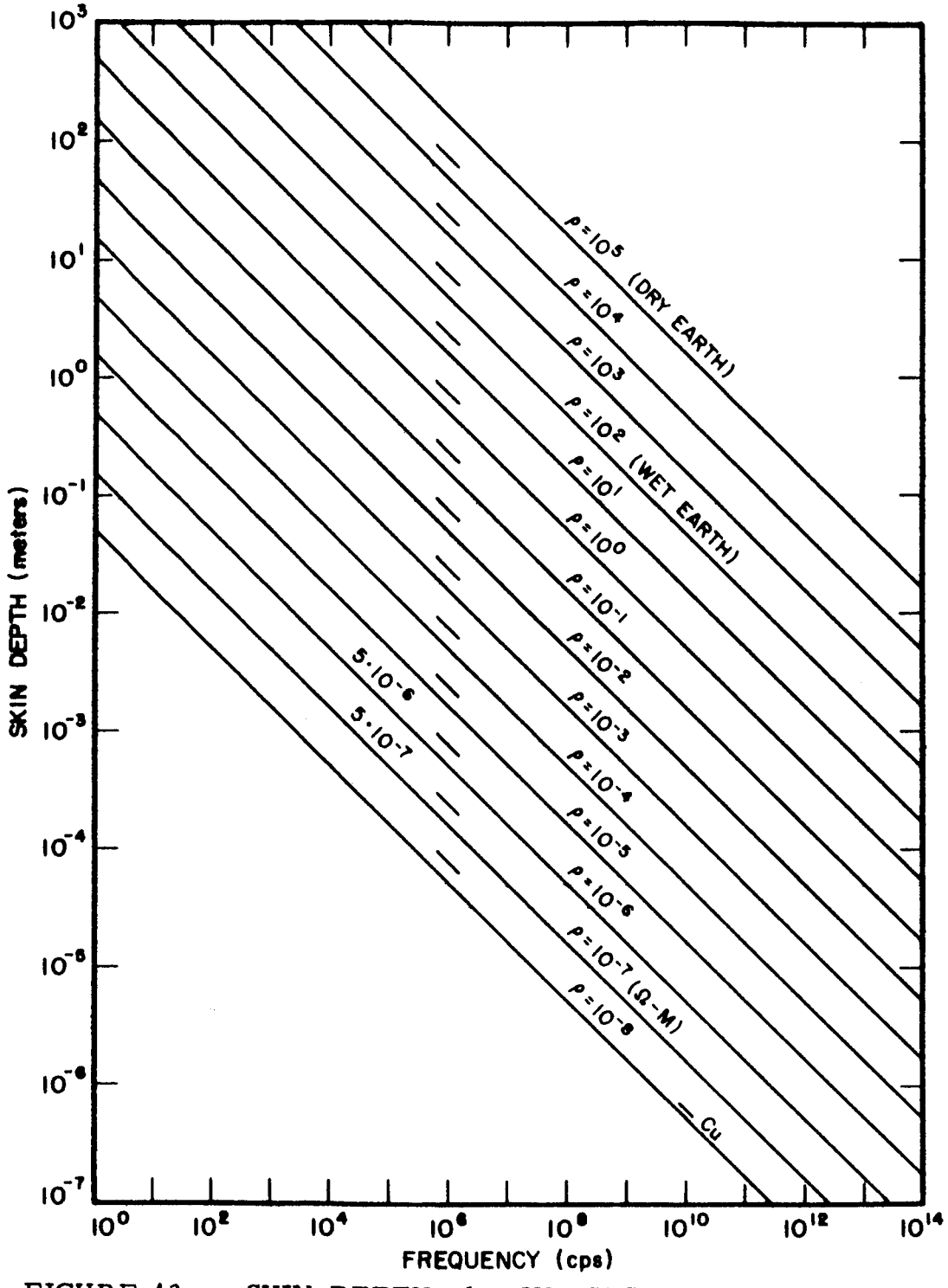

FIGURE 13 SKIN DEPTH, d_s, VERSUS FREQUENCY.

It is easily shown that, by Equation (77), if $(a/d_s) << 1$, then as $J_1(X) \doteq X/2$ and $J_o(X) \doteq 1$ for small X,

$$Z_\ell = \frac{1}{\pi a^2 \sigma} \quad , \tag{89}$$

which is just the dc resistance of the cylinder.

2. Cylindrical Capacitor

A most interesting problem in the consideration of diode resistance is the determination of the spreading resistance of the diode capacitor. This R_s is most critical in two diode capacitor applications. The first application is to the low noise parametric amplifier in which it represents the primary noise source. The second application is to the varactor (variable reactor) harmonic power generator. For the first application, the radius a of the contact is equal to or less than the skin depth in the metal wire contact and is much less than the skin depth in the semiconductor. In the second application, the radius of the contact surface is much greater than the skin depth of the metal contact and in most instances of practical importance can be considered to be much greater than the skin depth in the semiconductor also. This last statement must usually be qualified by closer consideration of the terminal frequencies involved as there may be as much as an order of magnitude difference between the signal and pump (and idler) frequencies of the parametric amplifier and also between the input and harmonic frequencies of the multiplier.

The question of the operation of the point contact diode will be put off until a later section. There it will be treated with the assumption of equipotential contact surface.

A complete formulation of the broad area contact problem is prohibitively complex but the important characteristics of the circular, back-biased junction may be derived by assuming it to be a circular, planar capacitor. Consider a capacitor consisting of two parallel circular plates of conductivity σ_1 and σ_2. The plates are separated by a narrow region of width $\underline{d}$ called the depletion layer (16) (17), the width of which we will assume to be determined and fixed by an applied reverse bias potential. This arrangement may be represented as shown in Figure 14.

The plates (1 and 2) have been shown as having different widths as well as different conductivities. The region 1 may approximate the large area (volume) dot or disk which would be used in the usual alloy junction forming process. The region 2 represents the basic semiconductor wafer. The region 3 then represents the regrowth (junction) location.

The $\underline{z}$ axis is the axis of symmetry, and it is safe to assume that the width of the depletion layer $\underline{d}$ is very small compared with either radius $\underline{a}$ or $\underline{b}$ and with the wavelength. That is

$$d \ll a \leq b \; ; \qquad d \ll \lambda \; ; \tag{90}$$

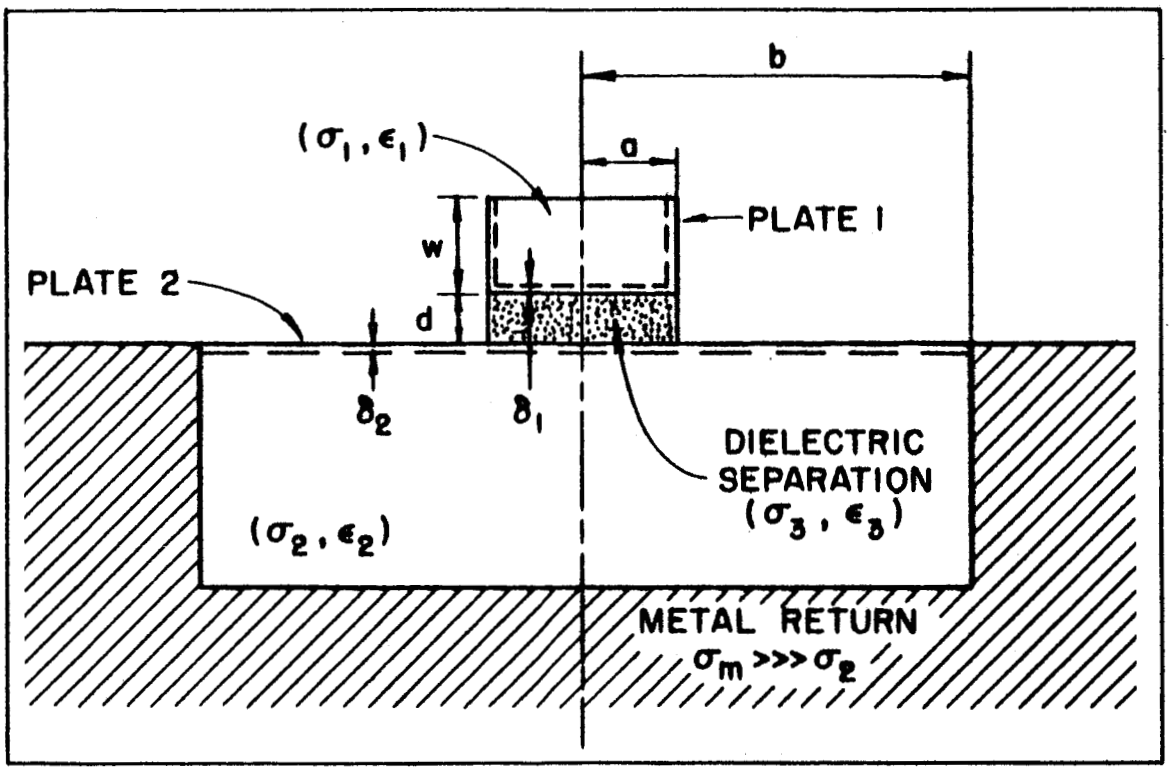

FIGURE 14 DIODE CAPACITOR REPRESENTATION.

hence, edge effects may be neglected, and the electric and magnetic intensities of region 3, E_{z3} and $H_{\theta 3}$, can be taken to be independent of $\underline{z}$, and Equations (70) and (71) hold, i.e.,

$$E_{z3}(r) = E_{z3}(a) \frac{J_o(\beta r)}{J_o(\beta a)} \quad , \tag{91}$$

and

$$H_{\theta 3}(r) = H_{\theta 3}(a) \frac{J_1(\beta r)}{J_1(\beta a)} \quad . \tag{92}$$

By application of the circuital law,

$$\oint_c H \cdot d\ell = (\sigma + j\omega\epsilon) \int_{s(cap)} E \cdot ds \quad , \tag{93}$$

the amplitudes $E_{z3}(a)$ and $H_{\theta 3}(a)$ may be obtained in terms of the total current I_{z1} entering or leaving the interface between regions 1 and 3. Thus

$$H_{\theta 3}(r) = \frac{I_{z1}}{2\pi a} \frac{J_1(\beta r)}{J_1(\beta a)} \quad , \tag{94}$$

and

$$E_{z3}(r) = \frac{j\omega\mu}{\gamma^2} \frac{I_{z1}}{\pi a^2} \left(\frac{\beta a}{2}\right) \frac{J_o(\beta r)}{J_1(\beta a)} \quad . \tag{95}$$

Now we have taken this to be the case, that the frequency is sufficiently high that the thickness of the plates and their radii are large compared to the skin depth (δ_1, δ_2) as shown in Figure 14. Then it may be assumed that most of the current flowing in region 1 flows in a thin layer, δ_1, radially, along the inner surface

of the conducting regions at the interface to region 3, around the edges and then axially (in region 1) just as was determined for the long cylindrical wire. Similarly the current flowing in region 2 flows in a thin layer δ_2 radially along the inner surface of the conducting region at the interface to region 3, and then directly radially to the return surface at r = b.

The radial current, $I_{r1}(r)$, at the interface can be determined by a second application of the circuital law by taking the cap surface to consist of a circular plate of radius r parallel to the interface of regions 1 and 3, but deep within region 1, and of a cylinder of radius r through which the radial current flows. As the plate is deep within the conductor (region 1) the integral over this surface is essentially zero. And then

$$H_{\theta 3}(r) = \frac{I_{r1}(r)}{2\pi r} \quad ; \tag{96}$$

but using Equation (94) we obtain

$$I_{r1}(r) = I_{z1}(\frac{r}{a}) \frac{J_1(\beta r)}{J_1(\beta a)} \quad , \tag{97}$$

which can be considered the total quasi-surface current flowing radially at the radius r. The surface current density, $I_r^s(r)$, is then defined as the total radial current traversing a unit circumference, i.e.,

$$I_r^s(r) = \frac{I_{z1}}{2\pi a} \frac{J_1(\beta r)}{J_1(\beta a)} \quad . \tag{98}$$

It has been shown[7], that when the above imposed conditions are satisfied, that a surface impedance may be derived for regions 1 and 2 which is

$$Z_s = \frac{1+j}{\sigma d_s} = R^s + jX^s \quad , \tag{99}$$

where d_s is again given by Equation (79), and that the average power dissipated per unit area of surface is Δp,

$$\Delta p = \frac{1}{2} R^s (I_r^s)^2 \quad . \tag{100}$$

Formula (100) is an expression for the I^2R loss which can be evaluated and to which an equivalent R_s can be assigned. The evaluation is performed in several parts. First the contribution to R_s (call it R_{13}^s) from only the interface between regions 1 and 3 is evaluated. Then that contribution, R_{32}^s, at the interface between regions 2 and 3 is similarly obtained. The contribution due to the axial flow in region 1, R_{ax}^s, is taken directly from Equation (88). The contribution due to the surface flow in region 2, but outside the radial limitation of r = a, is the final term, call it R_{sk}^s.

Then by Equations (98), (99), and (100), there is obtained

---

7. Reference (12), Chapter V, Section 13.

$$P = \frac{1}{2} \int_0^a R^s (I_r^s)^2 \, 2\pi r \, dr = \frac{1}{2} R_{13}^s I_{z1}^2 \quad . \tag{101}$$

The factor (1/2) is used before the second two terms because of the convention wherein I refers to peak quantities. Now R_{13}^s is obtained from Equation (101) and is found to be

$$R_{13}^s = \frac{1}{4\pi d_s \sigma_1} \left[1 + \frac{J_o^2(\beta a)}{J_1^2(\beta a)} \left(1 - \frac{2}{\beta a} \frac{J_1(\beta a)}{J_o(\beta a)} \right) \right] . \tag{102}$$

For the most important cases of application, it is valid to assume

$$\beta a << 1 \quad , \tag{103}$$

where upon we can use the Bessel function simplification for small arguments

$$J_o(X) \doteq 1 \tag{104}$$

and

$$J_1(X) \doteq \frac{X}{2} \tag{105}$$

to obtain for R_{13}^s the formula

$$R_{13}^s = \frac{1}{4\pi d_{s1} \sigma_1} \quad , \tag{106}$$

which has the surprising characteristic of being independent of the radius of the interface. It is obvious that the expression for R_{32}^s is similarly given.

$$R^s_{32} = \frac{1}{4\pi d_{s2}\sigma_2} \quad . \tag{107}$$

For expressions (106) and (107), σ_1 and σ_2 refer to the conductivities of regions 1 and 2 respectively; likewise d_{s1} and d_{s2} refer to the skin depths of regions 1 and 2 as evaluated by Equation (79). If the formula for d_s from Equation (79) be substituted into Equations (106) and (107), we obtain an expression for the total interface I^2R loss.

$$R^s_{13} + R^s_{32} = \frac{1}{4\pi}\left[\sqrt{\frac{\omega\mu_1}{2\sigma_1}} + \sqrt{\frac{\omega\mu_2}{2\sigma_2}}\right] \quad , \tag{108}$$

and here we note the similarity between this expression and the Rayleigh formula (87).

The contribution due to the flow of surface current in region 2, but for $r > a$, is obtained by substituting

$$I^s_r(r) = \frac{I_{z1}}{2\pi r} \tag{109}$$

into Equation (101); and again using R^s from Equation (99) we obtain

$$R^s_{sk} = \frac{1}{2\pi d_{s2}\sigma_2} \ln\left(\frac{b}{a}\right) \quad . \tag{110}$$

Finally, the total series resistance[8] of a large area varactor diode which can be represented by Figure 14 is given as

---

8. An expression for R_s for the broad area varactor was first presented by Hines (21). Details of his derivation are not available but is appears that only the interface contribution was considered. Hines gives

$$R_s = \frac{1}{8}\sqrt{\frac{f\mu}{\pi}}\left(\frac{1}{\sqrt{\sigma_1}} + \frac{1}{\sqrt{\sigma_2}}\right) .$$

$$R_s = \frac{1}{4\pi} \left\{ \sqrt{\frac{\omega\mu_1}{2\sigma_1}} \left(1 + \frac{2w}{a}\right) + \sqrt{\frac{\omega\mu_2}{2\sigma_2}} \left[1 + 2\ln\left(\frac{b}{a}\right)\right] \right\} . \qquad (111)$$

Equation (111) reflects the fact that we had previously made the assumption that the media of regions 1 and 2 are relatively good conductors. That is, the inequality

$$\frac{\omega\varepsilon}{\sigma} << 1 \qquad (112)$$

holds in both regions. Alternatively, it is said that the displacement currents are negligible when compared to the conduction currents.

The effect of non-negligible displacement currents will be discussed in a later section.

C. THE POINT CONTACT DIODE

Skin effect at a metal-semiconductor contact has already been briefly examined.[9] The intent of that examination was to determine the spatial distribution of current at the contact. A very simple model was considered. It consisted of two semi-infinite right circular cylinders, one of metal, the other of semiconductor having the same diameter as the metal, and connected coaxially with a nonrectifying butt joint. The results are given in reference to cylinders of diameters comparable to the diameter of the point of the practical point contact diode. It is shown that the redistribution of current flow lines from a decided skin effect

---

9. Reference (18) - Appendix B.

in the metal to a negligible effect in the semiconductor takes place mostly in the metal. Thereafter, it is concluded that, "the skin effect is entirely negligible for all point-contact rectifiers at any microwave frequency and the current flow at the contact may be treated with the dc approximation." Not considered was the fact that the current fans out in the semiconductor, and, when skin-effects set in, the total spreading resistance increases by the fan-out's becoming extreme to the point of crowding the current lines up to the surface of the semiconductor of a diode of the form of Figure 3.

This section will deal with the problem of the point contact diode, and we will derive a fairly rigorous expression for the spreading resistance which will include both frequency dependent (skin effect) terms and terms involving the semiconductor geometry. It will be further shown that the junction will definitely behave just as at dc, but that there is a significant correction to be made to R_s because of skin effect.

1. The Natural Coordinate System

The previously noted analysis and others which have similar configuration have contained drastic simplifications due to the complexity of exact analysis in cylindrical coordinates, which system, because of the physical configuration, one would consider the most applicable. But if one considers the dc case, it may be

shown that the oblate spheroidal coordinate system is the natural system as the current flow lines coincide with the coordinate system. Allow Figure 15 to define the coordinate system (19).

The rectangular (x, y, z) coordinates are related to the (ξ, η, ϕ) oblate spheroidal coordinates by the formulas

$$x = a\left[(1-\eta^2)(\xi^2+1)\right]^{1/2} \cos\phi \tag{113}$$

$$y = a\left[(1-\eta^2)(\xi^2+1)\right]^{1/2} \sin\phi \tag{114}$$

$$z = a\eta\xi \quad , \tag{115}$$

where

$$0 \le \eta \le 1, \; -\infty < \xi \le 0, \; 0 \le \phi \le 2\pi \quad .$$

The metrical coefficients are given as

$$h_1 = a\left(\frac{\xi^2+\eta^2}{\xi^2+1}\right)^{1/2} \quad , \tag{116}$$

$$h_2 = a\left(\frac{\xi^2+\eta^2}{1-\eta^2}\right)^{1/2} \quad , \tag{117}$$

and

$$r = a\left[(1-\eta^2)(\xi^2+1)\right]^{1/2} \quad . \tag{118}$$

Laplace's equation, $\nabla^2 V = 0$, is given in oblate spheroidal coordinates as

$$\left[\frac{\partial}{\partial\eta}(1-\eta^2)\frac{\partial}{\partial\eta} + \frac{\partial}{\partial\xi}(\xi^2+1)\frac{\partial}{\partial\xi}\right] V = 0 \quad , \tag{119}$$

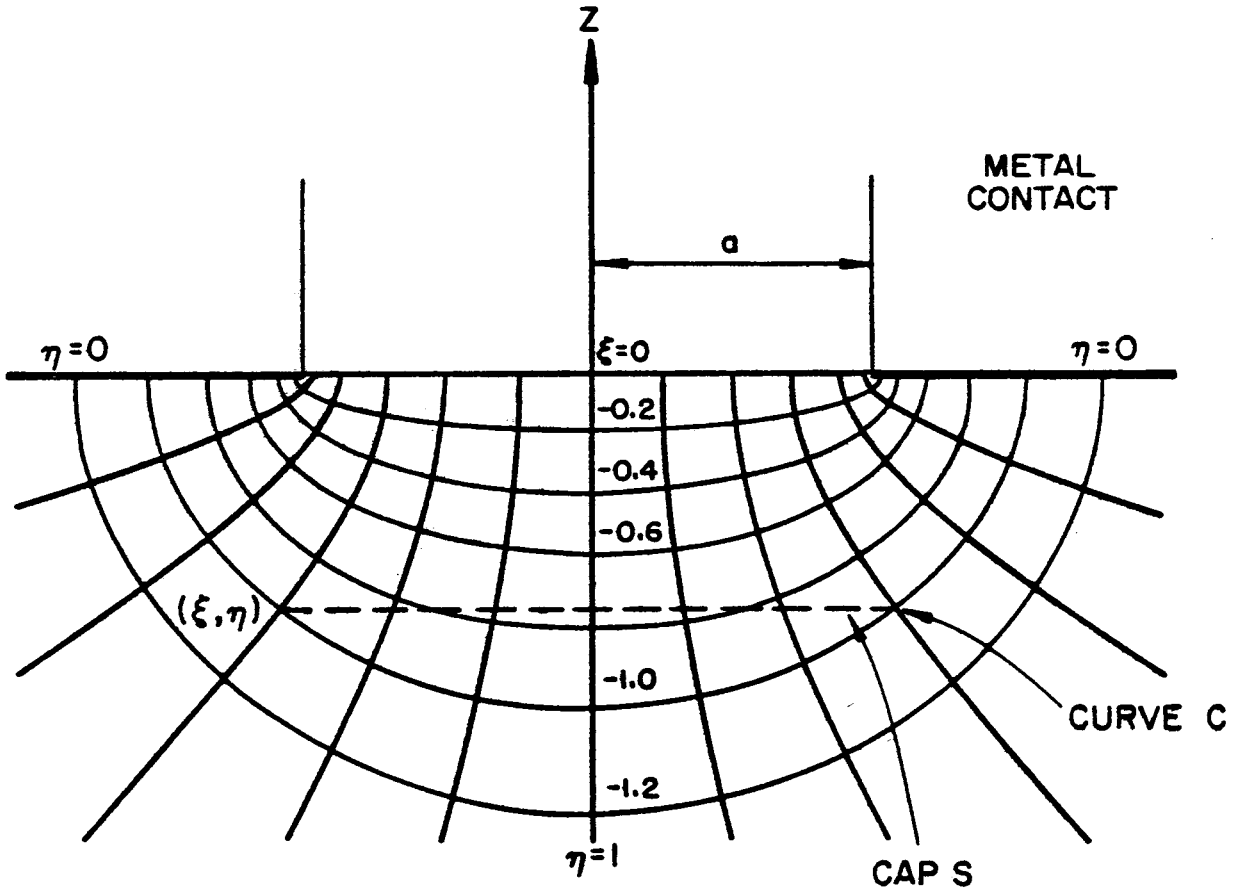

FIGURE 15 OBLATE SPHEROIDAL COORDINATE SYSTEM.

where the ϕ dependence has already been set equal to zero. The contact surface, taken to be the disk of radius $\underline{a}$ at $\xi = 0$, is at constant potential V_o. Since the contact disk is equipotential, then Laplace's equation shows that $(\partial V/\partial \eta) = 0$ must hold through the entire region and the potential V, must therefore be independent of η. Equation (119) then reduces to

$$\left[\frac{\partial}{\partial \xi}(\xi^2 + 1)\frac{\partial}{\partial \xi}\right] V = 0 \quad , \tag{120}$$

which has the solution of the form

$$V(\xi) = C_1 \tan^{-1} \xi + C_2 \quad , \tag{121}$$

where C_1 and C_2 are constants of integration. If we take $V = V_o$ at $\xi = 0$ and $V = 0$ at $\xi = -\infty$, it can be shown that

$$V(\xi) = V_o \left[1 + \frac{2}{\pi}\tan^{-1}\xi\right] \quad . \tag{122}$$

The current density is $J = -\sigma \nabla V$ which is

$$J = -\frac{\sigma}{h_1}\frac{\partial V(\xi)}{\partial \xi} \tag{123}$$

and by using Equations (116) and (122), J becomes at the disk electrode ($\xi = 0$)

$$J = \frac{-2V_o\sigma}{\pi a \eta} \quad . \tag{124}$$

Integrating this current density over the surface of the disk one obtains the total current I_T which allows the calculation of the spreading resistance $R_s = V_o/I_T$.

$$I_T = 4V_o \sigma a \tag{125}$$

Thus

$$R_s = \frac{1}{4\sigma a} \quad , \tag{126}$$

which agrees with the result previously obtained for the infinite half space (Equation 22). Likewise, if one solves Equation (118) for η when $\xi = 0$ and substitutes this into Equation (12 4), then Equation (19), representing the current density into the disk, is likewise verified.

2. Field Equations in the Oblate Spheroidal Systems

To extend these considerations to the determination of the skin effect, we return to the use of the scalar function Q. If the metrical coefficients as given in Equations (116), (117), and (118) are substituted into the differential Equation (58), there is obtained the differential equation for Q which must be satisfied when Q is described in the oblate spheroidal coordinate system,

$$(\xi^2+1)\frac{\partial^2 Q}{\partial \xi^2} + (1-\eta^2)\frac{\partial^2 Q}{2\eta^2} - a^2\gamma^2(\xi^2+\eta^2)Q = 0. \tag{127}$$

Use of

$$Q(\xi, \eta) = Q(\eta)Q(\xi) \tag{128}$$

to effect the separation of variables leads to the two differential equations, related only by the separation constant c, given by Equations (129) and (130),

$$(\xi^2+1)\frac{\partial^2 Q(\xi)}{\partial \xi^2} - (a^2\gamma^2\xi^2 + C)Q(\xi) = 0 \qquad (129)$$

and

$$(1-\eta^2)\frac{\partial^2 Q(\eta)}{\partial \eta^2} - (a^2\gamma^2\eta^2 - C)\,Q(\eta) = 0 \quad . \qquad (130)$$

Upon setting $C = a^2\gamma^2$, solutions for $Q(\xi)$ and $Q(\eta)$ may be obtained of the form

$$Q(\xi) = C_1 e^{a\gamma\xi} + C_2 e^{-a\gamma\xi} \qquad (131)$$

and

$$Q(\eta) = C_3 e^{ja\gamma\eta} + C_4 e^{-ja\gamma\eta} \quad . \qquad (132)$$

Further, we expect Q to have an exponential z dependence, and as $z = a\eta\xi$, it is easily shown that $Q(\xi, \eta)$ may also take the form

$$Q(\xi, \eta) = C_5 e^{a\gamma\eta\xi} + C_6 e^{-a\gamma\eta\xi} \quad . \qquad (133)$$

Therefore, a solution of Equation (127) could take the following form.

$$Q(\xi, \eta) = A_1 e^{a\gamma\eta\xi} + e^{a\gamma\xi}\left[A_2 e^{ja\gamma\eta} + A_3 e^{-ja\gamma\eta}\right] \quad , \qquad (134)$$

where the coefficients A_1, A_2, and A_3 are arbitrary constants, and the negative exponential has been dropped as we require Q to be finite as $\xi \to \infty$.

It is recognized that solutions of Equation (127) via the procedure of separation of variables and the use of Equations (129) and (130) are infinite in number and may be obtained in the form of Lamé products (19), but it will be shown that the form given in Equation (134) is sufficient to satisfy the boundary conditions on Q. Q is defined by Equation (55). By the circuital law we obtain the form of Q to be

$$Q(\xi, \eta) = \frac{I_T(\xi, \eta)}{2\pi} \quad , \tag{135}$$

where we have made use of the independence of $Q(\xi, \eta)$ from ϕ. $I_T(\xi, \eta)$ is the total current passing through the cap surface S, which is bounded by the curve C, which is a circle passing through the point (ξ, η) such that the cap S is normal to the $\underline{z}$ axis as shown in Figure 15.

If we take I_T to be the total current flowing across the surface ($\xi = 0$), then the following conditions apply and must be satisfied by $Q(\xi, \eta)$.

$$Q(\xi, 0) = \frac{I_T}{2\pi} \tag{136}$$

$$Q(\xi, 1) = 0 \tag{137}$$

$$Q(-\infty, \eta) = 0 \tag{138}$$

$$Q(-\infty, 0) = \frac{I_T}{2\pi} \tag{139}$$

These four conditions are satisfied by

$$Q(\xi, \eta) = \frac{I_T}{2\pi} \left[e^{a\gamma\eta\xi} - e^{a\gamma\xi} \frac{\sin(a\gamma\eta)}{\sin(a\gamma)} \right] . \qquad (140)$$

From Equations (56) and (57) the electric intensities are found to be

$$E_\xi(\xi, \eta) = \frac{j\omega\mu}{a\gamma} \frac{(I_T/2\pi)}{\sqrt{(\xi^2+1)(\xi^2+\eta^2)}} \left[\xi e^{a\gamma\eta\xi} - e^{a\gamma\xi} \frac{\cos(a\gamma\eta)}{\sin(a\gamma)} \right]. \qquad (141)$$

and

$$E_\eta(\xi, \eta) = \frac{-j\omega\mu}{a\gamma} \frac{(I_T/2\pi)}{\sqrt{(1-\eta^2)(\xi^2+\eta^2)}} \left[\eta e^{a\gamma\eta\xi} - e^{a\gamma\xi} \frac{\sin(a\gamma\eta)}{\sin(a\gamma)} \right]. \qquad (142)$$

3. Current Distribution

The current densities are given by

$$J_\xi(\xi, \eta) = \frac{a\gamma I_T}{2\pi a^2} \frac{1}{\sqrt{(\xi^2+1)(\xi^2+\eta^2)}} \left[\xi e^{a\gamma\eta\xi} - e^{a\gamma\xi} \frac{\cos(a\gamma\eta)}{\sin(a\gamma)} \right] \qquad (143)$$

and

$$J_\eta(\xi, \eta) = \frac{-a\gamma I_T}{2\pi a^2} \frac{1}{\sqrt{(1-\eta^2)(\xi^2+\eta^2)}} \left[\eta e^{a\gamma\eta\xi} - e^{a\gamma\xi} \frac{\sin(a\gamma\eta)}{\sin(a\gamma)} \right] . \qquad (144)$$

Equations (143) and (144) were evaluated at the contact surface $\xi = 0$. An average current density, $\bar{J} = I_T/\pi a^2$, is defined after which the ratios $J_\xi/\bar{J}$ and $J_\eta/\bar{J}$ were calculated for various points across the contact and the results plotted versus (r/a), the fractional radius. Again the assumption is made that the material is a relatively good conductor. Then as

$$a\gamma = (1 + j)\frac{a}{d_s} \quad , \tag{145}$$

where d_s is from Equation (79), the normalized current densities can be plotted as a function of the ratio a/d_s, which is the ratio of contact radius to bulk material skin depth. Figures 16 and 17 show J_η/J and J_ξ/J respectively for three values of a/d_s. But note in each case (as was calculated) there was no significant difference between the case for $(a/d_s) = 0.25$ and $(a/d_s) = 0$. The latter case obviously is the dc case, and the curve of J_ξ/J is just that which would be obtained by plotting Equation (124) versus r/a. But the case (which does not measurably differ from the dc case) $(a/d_s) = 0.25$ corresponds to an extreme case determined by the conditions:

i) frequency of 50 Gc.

ii) A contact radius a = 0.05 mil. This is representative of typical microwave and millimeter wave point contact diodes (3) (18).

iii) Bulk semiconductor resistivity $\rho = 0.0005$ ohm-cm.

This figure represents the resistivity that would be encountered in millimeter wave tunnel diodes and is from one to two orders of magnitude lower than that encountered in the more conventional point contact diodes.

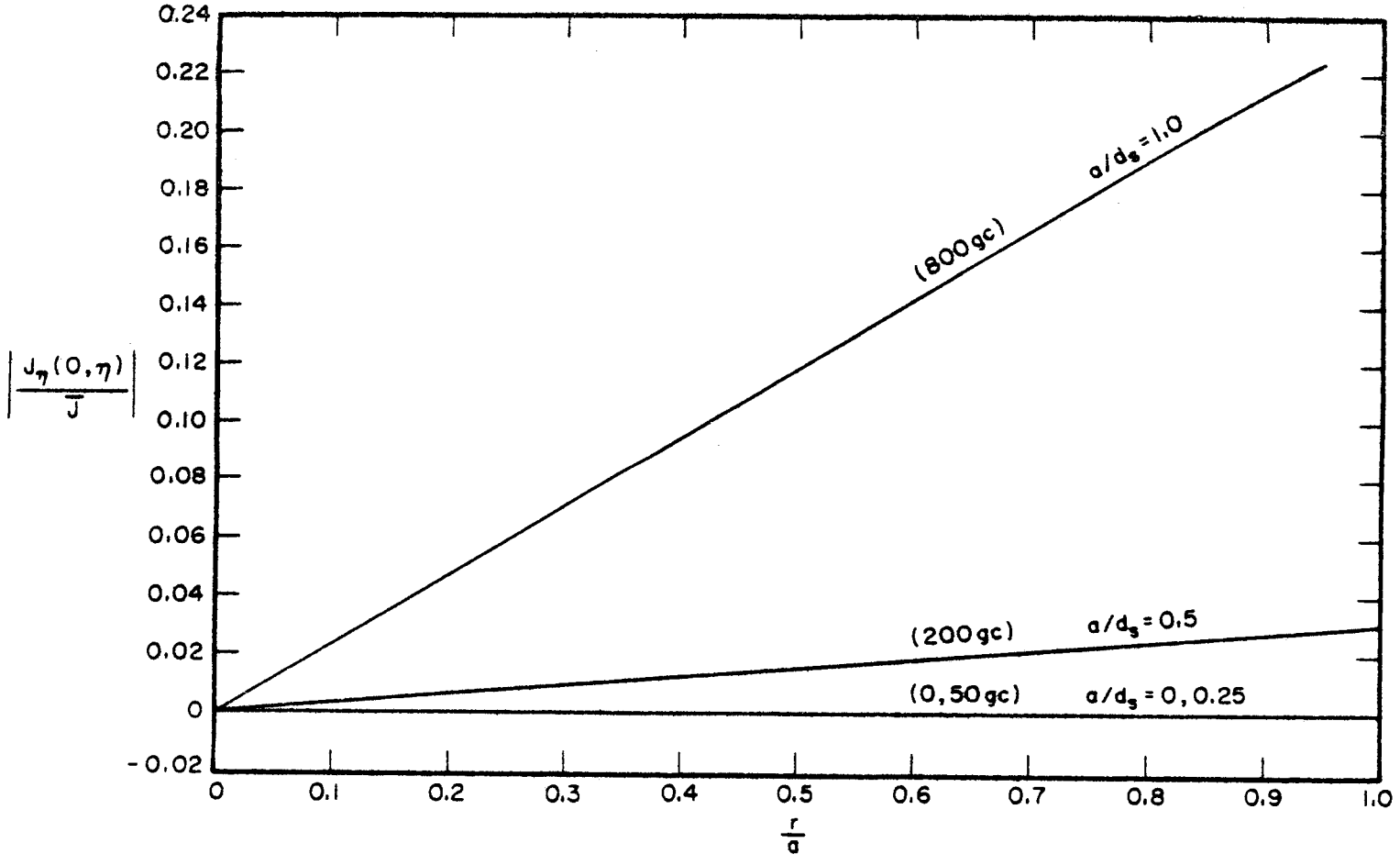

FIGURE 16 NORMALIZED RADIAL CURRENT DENSITY VERSUS FRACTIONAL RADIUS.

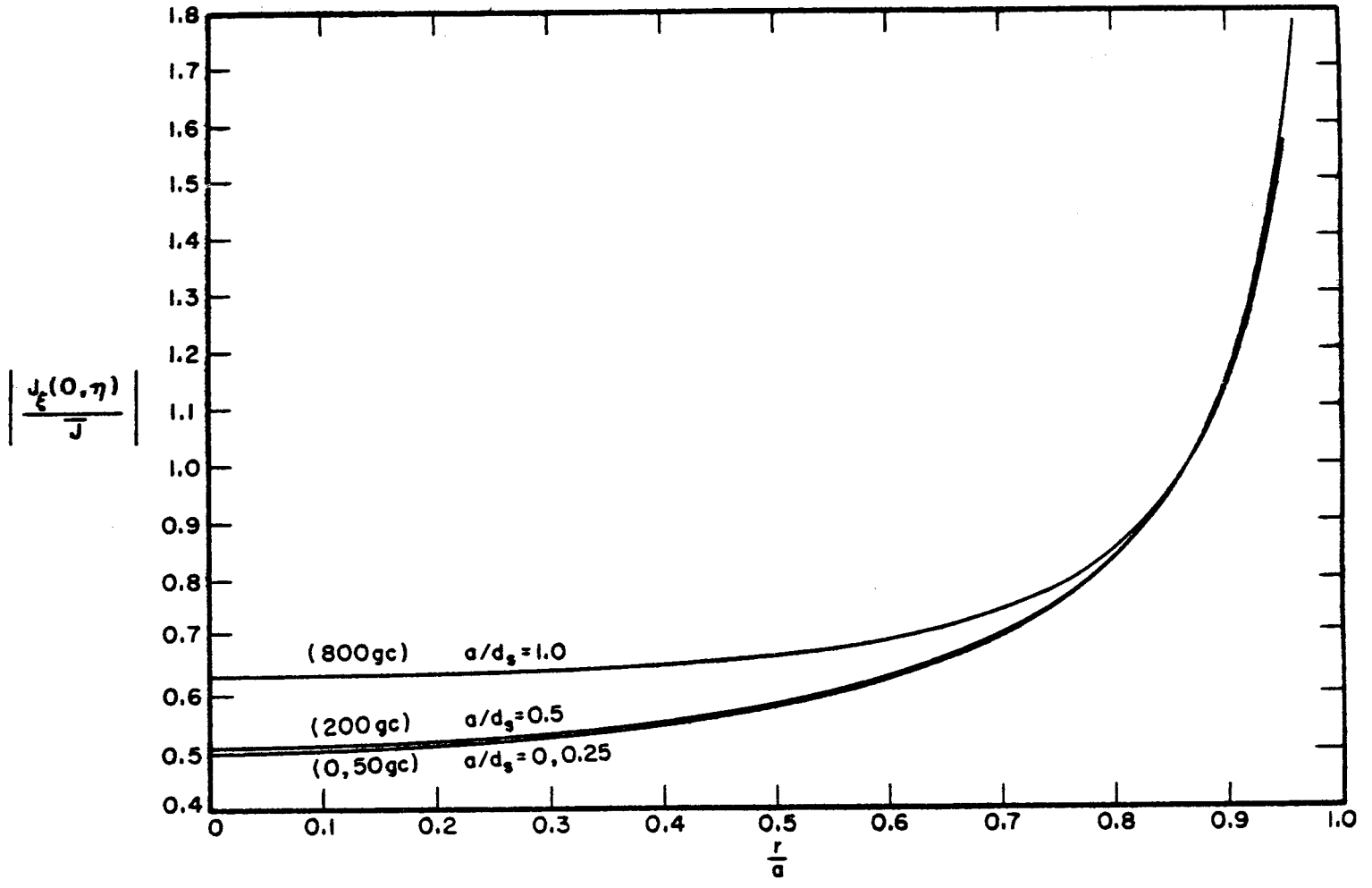

FIGURE 17 NORMALIZED AXIAL CURRENT DENSITY J_ξ VERSUS FRACTIONAL RADIUS.

Inspection of the curve for J_η shows that essentially $J_\eta = 0$ for $(a/d_s) \leq 0.25$ and becomes measurable only when $(a/d_s) \doteq 0.5$. But for the same conditions as in ii) and iii) above, this (a/d_s) ratio corresponds to a frequency range of 200 Gc. Further, as the I^2R contribution due to J_η will be less than 0.1 per cent of that due to J_ξ, it would appear that even to this extreme value of (a/d_s) the current density expressions are good, and the contact still represents an equipotential.

The curves for $(a/d_s) = 1.0$ show much more deviation for J_η, and its I^2R contribution now becomes about 5 per cent. But this figure, $(a/d_s) = 1.0$, corresponds to a frequency of 800 Gc which is quite beyond the range of anticipated application of these results.

In addition to the curves for J_η and J_ξ, the curves showing the actual current distribution are shown in Figure 18. In this figure $I(r/a)$ is the total current entering the electrode in a circle of radius r. This is then normalized to the total current I_T. Notice that the curves for $(a/d_s) = 0$, 0.25, and 0.5 essentially coincide (within the plotting ability), and that no appreciable redistribution of the current occurs until (a/d_s) becomes greater than 0.5. The data for $(a/d_s) = 1$, which corresponds to a frequency of 800 Gc for this case, begin to show deviations, but are still far below the curve shown for the case of constant current density.

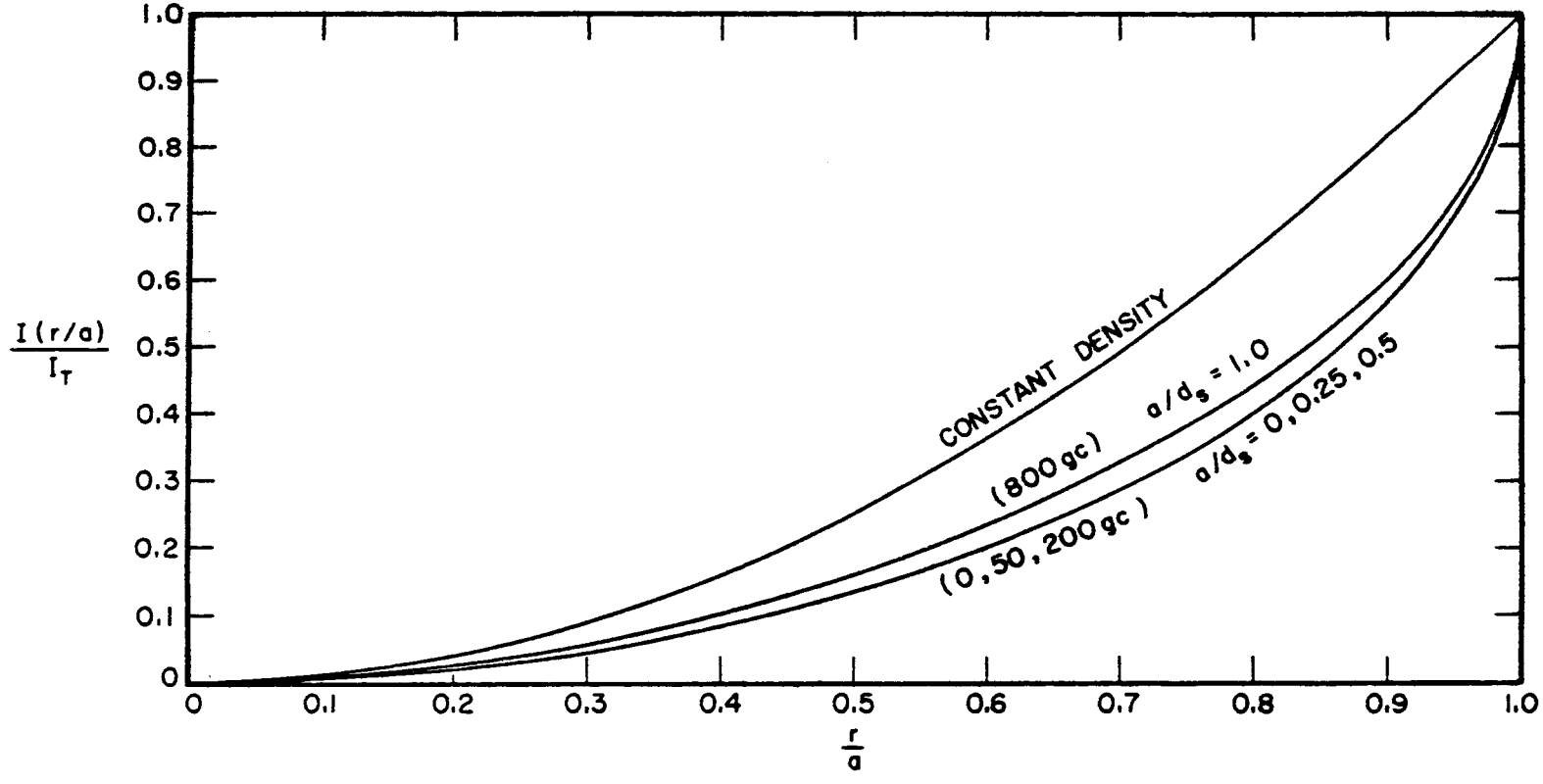

FIGURE 18 NORMALIZED TOTAL CURRENT DISTRIBUTION I(r/a) VERSUS FRACTIONAL RADIUS.

With this development and this discussion it is believed that the statement, " at the junction, the current flow may be treated with the dc approximation", has been sufficiently rigorously proven. In addition, meaning is given to the statement, because now the equations exist which allow the evaluation of the associated spreading resistance, and make it unnecessary to assume that, because the junction can be treated with the dc approximation, the rest of the problem can be also.

4. Spreading Resistance

To obtain the spreading resistance with the skin effect contribution the following assumption will be made; that the wafer of semiconductor material, rather than being considered the infinite half-space, have a definite radius b, and that the thickness of the wafer be appreciably greater than the skin depth in the wafer. Except for diodes constructed on epitaxial materials this is a good assumption. Allow Figure 19 to show the situation. Region 1 represents the metal point contact. Region 2 is the semiconductor buried in the metal, high conductance return path 3. If the metal regions are of sufficiently high conductance relative to the semiconductor, then the principal potential drop will be across the semiconductor. If the expressions for the electric intensities (141) and (142) are examined, it can be seen that, for $\xi >> 1$ and for $z = 0$ ($a\eta\xi = 0$), E_η vanishes and that near the semiconductor

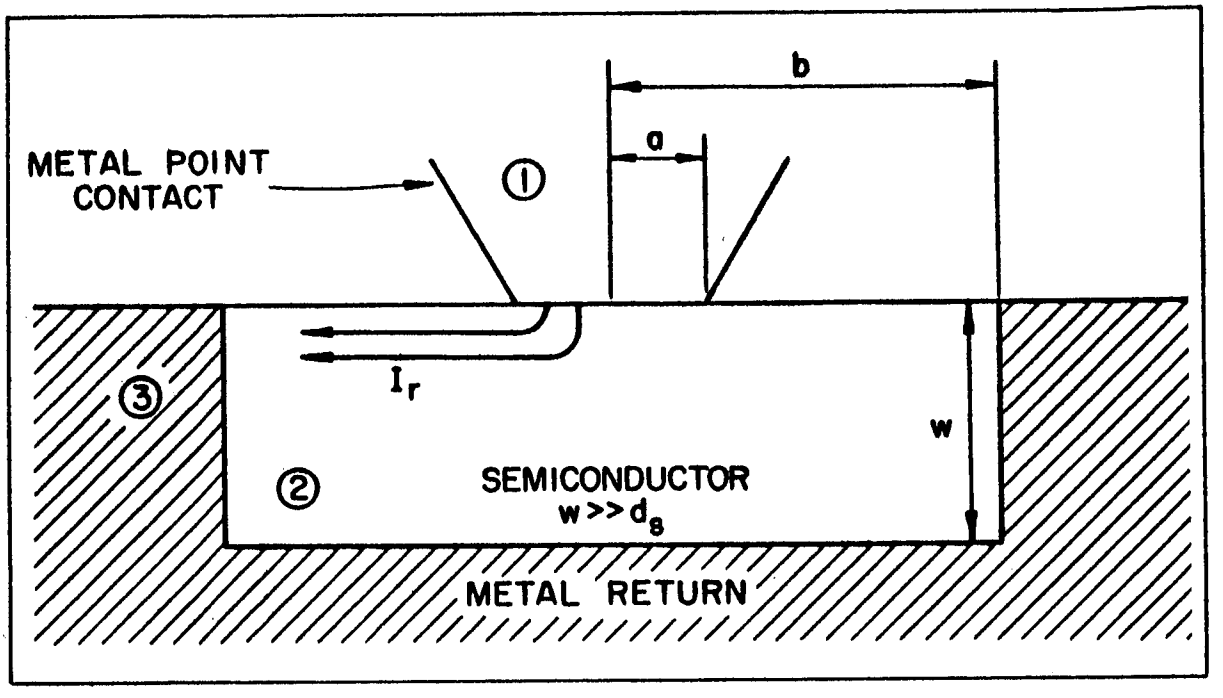

FIGURE 19 POINT CONTACT WITH SKIN EFFECT.

surface the current flow, I_r, becomes strictly radial as illustrated in Figure 19; hence the validity and necessity of applying the realistic condition at r = b. The potential drop across the semiconductor from r = a to r = b can be taken as

$$V = -\int_b^a E_\xi(\xi, 0)\, dr \quad , \tag{146}$$

where the integration proceeds along any one radial line because of the cylindrical symmetry of the situation. By Equation (118), for $\eta = 0$

$$r = a\sqrt{\xi^2 + 1} \rightarrow dr = \frac{a\xi d\xi}{\sqrt{\xi^2+1}} \quad , \tag{147}$$

and V is evaluated by Equation (146) by

$$V = -\frac{j\omega\mu}{\gamma}\frac{I_T}{2\pi}\left\{\int_{\xi_1}^{o} \frac{\xi d\xi}{\xi^2+1} - \frac{1}{\sin(a\gamma)}\int_{\xi_1}^{o} \frac{e^{a\gamma\xi}}{\xi^2+1}\, d\xi\right\}, \tag{148}$$

where

$$\xi_1 = -\left[\left(\frac{b}{a}\right)^2 - 1\right]^{1/2} \quad . \tag{149}$$

Call the first and second integrals of Equation (148) I_1 and I_2 respectively. I_1 is integrated directly and found to be

$$I_1 = -\ln\left(\frac{b}{a}\right) \quad . \tag{150}$$

Calculation of I_2 is a bit more troublesome. Substituting $\xi = -t$ and $a\gamma = s$ into I_2 yields

$$I_2 = \int_o^{b/a} \left(\frac{1}{t^2+1}\right)e^{-st}\, dt \quad , \tag{151}$$

where in the upper limit $\left[\left(\frac{b}{a}\right)^2 - 1\right]^{1/2}$ the one was dropped, as the ratio (b/a) is typically equal to or greater than 200. Because of the size (b/a) we can, for all intents and purposes, set the upper limit equal to $+\infty$, whereupon we find that I_2 is now the Laplace transform of the classical function known as the Witch of Agnesi (20). The transform of this function is given in terms of sines, cosines, and sine and cosine integrals. Thus,

$$I_2 = \left[\frac{\pi}{2} - \mathrm{Si}(a\gamma)\right] \cos(a\gamma) + \mathrm{Ci}(a\gamma) \sin(a\gamma) \quad . \tag{152}$$

Equation (152) is not particularly tractable, but by use of series expansions for the functions Si(X) and Ci(X), evaluation of I_2 could be accomplished. However, for most applications (a/d_s) is sufficiently small that the exponential of the integrand of Equation (151) may be considered essentially zero; then

$$I_2 \triangleq \tan^{-1}\left(\frac{b}{a}\right) \quad . \tag{153}$$

The impedance is then found to be

$$Z \triangleq \frac{(1+j)}{2\pi\sigma d_s} \ln\left(\frac{b}{a}\right) + \frac{1}{2\pi\sigma a} \tan^{-1}\left(\frac{b}{a}\right) \quad . \tag{154}$$

Agreement is obtained with the dc case with infinite half space of semiconductor, by noting that as $(b/a) \to \infty$ and frequency $\omega \to 0$ we have

$$\tan^{-1}\left(\frac{b}{a}\right) \to \frac{\pi}{2} \text{ as } \left(\frac{b}{a}\right) \to \infty \tag{155}$$

and

$$d_s \to \infty \text{ as } \omega \to 0 \quad , \tag{156}$$

yielding, in the limit

$$\lim_{\substack{\omega \to 0 \\ \frac{b}{a} \to \infty}} Z = \frac{1}{4\sigma a} \quad , \tag{157}$$

which agrees with Equation (126).

The real part of Z can now be taken to be the total spreading resistance, R_s, of the device shown in Figure 19. Thus

$$R_s = \frac{1}{2\pi\sigma} \left[\frac{1}{d_s} \ln \left(\frac{b}{a}\right) + \frac{1}{a} \tan^{-1} \left(\frac{b}{a}\right) \right] \quad , \tag{158}$$

and

$$R_s = \frac{1}{2\pi} \left[\sqrt{\frac{\omega\mu}{2\sigma}} \ln \left(\frac{b}{a}\right) + \frac{1}{\sigma a} \tan^{-1} \left(\frac{b}{a}\right) \right] . \tag{159}$$

IV. CONDUCTION CURRENTS VERSUS DISPLACEMENT CURRENTS

In all the calculations and discussions in the paper involving the skin depth d_s, the assumption has been made that the region of interest was composed of a "reasonably" good conductor, and thus the ratio, β, of the magnitudes of the displacement to conduction currents was taken to be zero. If such is not the case the attenuation term, $\mathrm{Re}\{\gamma z\}$, must be re-examined. If we call δ the true skin depth then

$$\delta = \frac{1}{\mathrm{Re}\{\gamma\}} \quad . \tag{160}$$

As γ is the intrinsic propagation constant then γ^2 is given by

$$\gamma^2 = j\omega\mu\,(\sigma + j\omega\epsilon) \tag{161}$$

and for $\mathrm{Re}\{\gamma\}$ it may be shown that

$$\mathrm{Re}\{\gamma\} = \frac{\sqrt{2}}{d_s}\,(1+\beta^2)^{1/4} \cos\left[\frac{1}{2}\left(\frac{\pi}{2} + \tan^{-1}\beta\right)\right] , \tag{162}$$

where β is defined to be

$$\beta = \frac{\omega\epsilon}{\sigma} \quad , \tag{163}$$

where $\epsilon = \epsilon_o\epsilon_r$, in which ϵ_o and ϵ_r are the permittivity of free space and the relative permittivity (dielectric constant) respectively. σ, as was defined previously, is the conductivity of the material, d_s is the skin depth (Equation (79)) as calculated for $\beta = 0$, and shown in Figure 13.

Now the true skin depth, δ, is given by

$$\delta = K_\beta d_s \quad , \tag{164}$$

where the scale factor K_β is taken from Equation (162) and is

$$K_\beta = \left\{ \sqrt{2}\,(1+\beta^2)^{1/4} \cos\left[\tfrac{1}{2}\left(\tfrac{\pi}{2} + \tan^{-1}\beta\right)\right] \right\}^{-1}. \tag{165}$$

K_β is plotted versus β and presented in Figure 20. In all the cases where the term d_s was used, if it be necessary, the corrected term δ may be obtained by evaluating K_β (reading from Figure 20) and scaling d_s accordingly. In all cases, the skin effect term of the spreading resistance is inversely proportional to K_β, and thus the correction applies directly to the resistance term.

To demonstrate the general range of β, we compute for a semiconductor of $\epsilon_r = 16$ and conductivity $\sigma = 1$ mho/cm and a frequency of 100 Gc, and obtain $\beta \doteq 1.0$. For these conditions the true skin depth δ will be about 60 per cent greater than that value d_s, normally used. But it should also be pointed out that a very high frequency was taken and that the material resistivity was at least one order of magnitude too high for the usual millimeter wave point-contact diode and as much as three orders of magnitude higher than the resistivity needed for the fabrication of high frequency point-contact tunnel diodes. By these arguments it is seen that for most high frequency diode calculations the correction need not be applied. Similar arguments apply when the spreading resistance with skin effect is being considered in a transistor. While

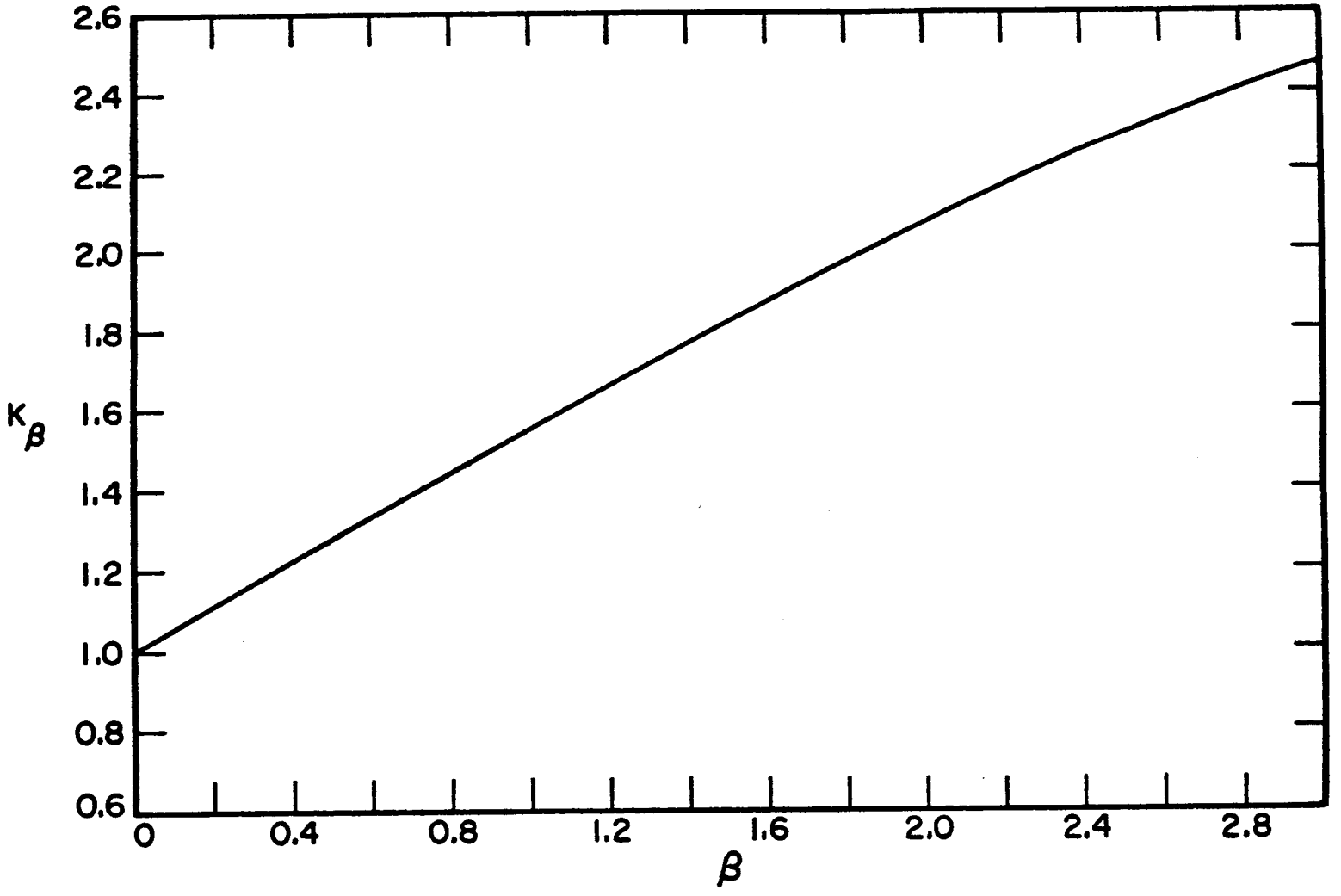

FIGURE 20 SCALE FACTOR, K_β DUE TO NON-NEGLIGIBLE DISPLACEMENT CURRENT.

the resistivity of the transistor material may be one to two orders of magnitude higher than in a microwave diode, the frequency of operation is usually two to three orders of magnitude less than the 100 Gc figure used here. Again the correction term should prove negligible.

V. CONCLUSIONS

The dc spreading resistance has been calculated specifically for the constant current distribution and the current distribution of the disk electrode over an infinite half space. The calculations were performed for a large range of the geometrical parameters (a/b) and (w/b). The data have been presented in Figures 7, 8, 9, and 10.

Presented also are "composite" curves which are applicable to almost any case wherein the disk electrode is a direct contact and is an equipotential. The composite curves are presented in Figures 11 and 12. A discussion of the limitations of applicability of these curves is given at the end of Section V.

Equations for the spreading resistance of the broad area variable capacitance diode and the point contact variable resistance diode have been derived in terms of frequency, material characteristics (μ, ϵ, σ), and physical parameters (b/a) and (w/a). The results are presented in Equations (111) and (159).

The field equations for the point contact diode configuration have been derived in terms of the oblate spheroidal coordinates. It has been shown that this is the natural coordinate system for such an analysis and that the spreading resistance is quite readily derived in this system.

A discussion is presented which shows that the effects of displacement current in the semiconductor are, in most instances, negligible in comparison to the conduction currents.

The author claims the following features to be the contributions of importance to the literature of electrical (semiconductor) engineering:

i) The graphs of Figures 7 through 12, presenting data which are easily used to determine the low frequency diode spreading resistance, R_s, for a wide range of parameters.

ii) The detailing of the methods of treating the skin effects in capacitor diodes.

iii) The derivation of the field equations and the resulting spreading resistance of the point contact device.

REFERENCES

1. Uhlir, A., Jr., "The Potential of Semiconductor Diodes in High Frequency Communications," Proc. IRE, Vol. 46, June 1958.

2. Sharpless, W. M., "Wafer-Type Millimeter Wave Rectifiers," BSTJ, Vol. 35, November 1956.

3. Sharpless, W. M., "Gallium-Arsenide Point Contact Diodes," IRE Trans. on MTT, Vol. 9, January 1961.

4. DeLoach, B. C., "17.35 and 30 Kmc Parametric Amplifiers," Proc. IRE, Vol. 48, July 1960.

5. Weber, H., "Ueber Bessel'sche Functionen und ihre Anwendung auf die theorie der elektrischen Ströme," Crelle, Bd. 75, 1873.

6. Gray, A. and Mathews, G. B., A Treatise on Bessel Functions, New York, MacMillan and Co., 1895.

7. Windred, G., Electrical Contacts, London, MacMillan and Co., Ltd., 1940.

8. Holm, R., Electric Contacts, Stockholm, Hugo Gebers Förlag, 1946.

9. Sackett, W. T., Jr., Contact Resistance, Dissertation, Department of Electrical Engineering, School of Engineering Science, The Johns Hopkins University, 1950.

10. Hagner, D. R., Multiple Contact Resistance, Dissertation, Department of Electrical Engineering, School of Engineering Science, The Johns Hopkins University, 1953.

11. Kennedy, D. P., "Spreading Resistance in Cylindrical Semiconductor Devices," J.A.P., Vol. 31, August 1960.

12. King, R. W. P., Electromagnetic Engineering, New York, McGraw-Hill Book Co., Inc., 1945.

13. Smythe, W. R., "Current Flow in Cylinders," J.A.P., Vol. 24, January 1953.

14. Stratton, J. A., Electromagnetic Theory, New York, McGraw-Hill Book Co., 1941.

15. Jahnke, E. and Emde, F., Tables of Functions, New York, Dover Publications, 1945.

16. Blackwell, L. A., and Kotzebue, K. L., Semiconductor-Diode Parametric Amplifiers, New Jersey, Prentice-Hall, Inc., 1961.

17. Chang, K. K. N., Parametric and Tunnel Diodes, New Jersey, Prentice-Hall, Inc., 1964.

18. Torrey, H. C., and Whitmer, C. A., Crystal Rectifiers, New York, McGraw-Hill Book Co., Inc., 1948.

19. Flammer, C., Spheroidal Wave Functions, A Stanford Research Institute Monograph, Stanford University Press, 1957.

20. Korn, G. A., and Korn, T. M., Mathematical Handbook for Scientists and Engineers, New York, McGraw-Hill Book Co., Inc. 1961.

21. Hines, M. E., "High Frequency Limitations of Solid-State Devices and Circuits," A Discourse presented to the 1963 International Solid State Circuits Conference, University of Pennsylvania, Philadelphia, Pennsylvania.